Author Manuscript

Author Manuscript

Author Manuscript

Author Manuscript

HHS Public Access

Author manuscript

J Neuropathol Exp Neurol. Author manuscript; available in PMC 2016 November 01.

Published in final edited form as:

J Neuropathol Exp Neurol. 2015 November ; 74(11): 1093–1118. doi:10.1097/NEN.0000000000000255.

Altered Oligodendrocyte Maturation and Myelin Maintenance: The Role of Anti-Retrovirals in HIV-Associated Neurocognitive Disorders

Brigid K. Jensen, BS[1,2,3], **Hubert Monnerie, PhD**[2], **Maggie V. Mannell, MS**[1], **Patrick J. Gannon, PhD**[3], **Cagla Akay Espinoza, MD**[3], **Michelle A. Erickson, PhD**[3], **Annadora J. Bruce-Keller, PhD**[4], **Benjamin B. Gelman, MD, PhD**[5], **Lisa A. Briand, PhD**[6], **R. Christopher Pierce, PhD**[7], **Kelly L. Jordan-Sciutto, PhD**[3], and **Judith B. Grinspan, PhD**[2]

[1]Department of Neuroscience, The Perelman School of Medicine, University of Pennsylvania, Philadelphia, Pennsylvania

[2]Department of Neurology, The Children's Hospital of Philadelphia, Philadelphia, Pennsylvania

[3]Department of Pathology, School of Dental Medicine, University of Pennsylvania, Philadelphia, Pennsylvania

[4]Pennington Biomedical Research Center, Louisiana State University System, Baton Rouge, Louisiana

[5]Department of Pathology, University of Texas Medical Branch, Galveston, Texas

[6]Department of Psychology, College of Liberal Arts, Temple University, Philadelphia, Pennsylvania

[7]Center for Neurobiology and Behavior, Department of Psychiatry, The Perelman School of Medicine, University of Pennsylvania, Philadelphia, Pennsylvania

Abstract

Despite effective viral suppression through combined antiretroviral therapy (cART), approximately half of HIV-positive individuals suffer from HIV-Associated Neurocognitive Disorders (HAND). Studies of antiretroviral treated patients have revealed persistent white matter pathologies including diffuse myelin pallor, diminished white matter tracts, and decreased myelin protein mRNAs. Loss of myelin can contribute to neurocognitive dysfunction as the myelin membrane generated by oligodendrocytes is essential for rapid signal transduction and axonal maintenance. We hypothesized that myelin changes in HAND are partly due to effects of antiretroviral drugs on oligodendrocyte survival and/or maturation. We showed that primary mouse oligodendrocyte precursor cell cultures treated with therapeutic concentrations of HIV protease inhibitors Ritonavir or Lopinavir displayed dose-dependent decreases in oligodendrocyte maturation; however, this effect was rapidly reversed following drug removal. Conversely,

Send correspondence and reprint requests to: Dr. Judith B. Grinspan, PhD, Professor, Department of Neurology, The Children's Hospital of Philadelphia, The Perelman School of Medicine at the University of Pennsylvania, 516D Abramson Center, 3615 Civic Center Blvd., Philadelphia, PA 19104. Tel: 215-590-2094; FAX: 215-590-3709; Grinspan@email.chop.edu.
Drs. Jordan-Sciutto and Grinspan contributed equally to this work.

Conflict of interest: The authors declare no competing financial interests

Author Manuscript Author Manuscript Author Manuscript Author Manuscript

nucleoside reverse transcriptase inhibitor Zidovudine had no effect. Furthermore, in vivo Ritonavir administration to adult mice reduced frontal cortex myelin protein levels. Finally, prefrontal cortex tissue from HIV-positive individuals with HAND on cART showed a significant decrease in myelin basic protein compared with untreated HIV-positive individuals with HAND or HIV-negative controls. These findings demonstrate that antiretrovirals can impact myelin integrity, and have implications for myelination in juvenile HIV patients, and myelin maintenance in adults on lifelong therapy.

Keywords

Antiretroviral; oligodendrocyte; myelin; HIV; HIV-Associated Neurocognitive Disorders; pediatric AIDS; Protease Inhibitor

INTRODUCTION

Approximately 50% of patients infected with human immunodeficiency virus-1 (HIV) present with a broad spectrum of cognitive, motor, and behavioral disturbances collectively termed HIV-Associated Neurocognitive Disorders (HAND) (1, 2) despite effective viral control through combined antiretroviral therapy (cART) (3–6). cART is designed to target multiple stages of HIV replication simultaneously, thereby delaying viral mutational selection to acquire drug resistance. Most commonly prescribed regimens include viral reverse transcriptase inhibitors (nucleoside/nucleotide reverse-transcriptase inhibitors [NRTIs]), and HIV protease inhibitors (PIs), which prevent maturation of viral precursor proteins (7). While cART successfully reduces peripheral viral loads to undetectable levels in adherent individuals, inflammation and latent viral reservoirs remain in the central nervous system (CNS) (8–12).

Although the pathological findings have shifted from subcortical to cortical manifestations since the introduction of cART, dendritic pruning and astrogliosis persist (4, 6, 13, 14). Notably, white matter abnormalities are prevalent and the degree of neurocognitive impairment has been correlated with the amount of damage (15, 16). Imaging studies have also revealed cortical myelin disruption, volume loss, and diminished structural integrity of the corpus callosum in HAND patients, which were even more pronounced in cART-treated individuals (17–19). Furthermore, transcriptome analysis in HAND patients on cART revealed dysregulation of genes critical to oligodendrocyte maturation and myelination, including myelin-associated oligodendrocyte basic protein, myelin transcription factor 1, and myelin basic protein (MBP) (20).

In pediatric HIV patients, neurological complications such as encephalopathy and progressive multifocal leukoencephalopathy are frequent and data suggest emerging neurocognitive deficits and developmental delays (21–23). World Health Organization (WHO) guidelines urge that all infected children be treated, with those under 3 years of age receiving a Lopinavir/Ritonavir first-line regimen (7). Importantly, this PI-based therapy is advised during the critical period for myelination (24), but an understanding of the effects of HIV and antiretroviral drugs on myelin formation and maintenance is lacking.

Author Manuscript Author Manuscript Author Manuscript Author Manuscript

The myelin membrane is critical for axons to transmit rapid neuronal impulses as well as axonal maintenance (25, 26). Conversely, impaired myelination can disrupt proper signaling and hasten axonal degeneration resulting in neurological dysfunction (27, 28). Although sustained effects of continuing viral replication and treatment noncompliance are suggested to underlie continuing neurocognitive impairment, antiretrovirals themselves may contribute to the pathogenesis of HAND (29–31). Crucially, while antiretroviral-mediated toxicity has been reported in primary rat cortical neurons (32, 33), to date there are no published studies addressing the effects of antiretrovirals on oligodendrocytes, the myelin forming cells of the CNS. Here we examine whether antiretrovirals affect the survival and maturation of developing oligodendrocytes using a well-established primary mouse cortical cell culture model (34) and the effects of cART compounds on myelin maintenance in a mouse model and in patients with HAND. Our results support a role for a subset of cART agents in the white matter changes seen in HIV-positive individuals with HAND.

MATERIALS AND METHODS

Chemicals and Reagents

Rabbit polyclonal anti-inositol-requiring enzyme 1 antibody (IRE1α, ab37073), rabbit polyclonal anti-inositol-requiring enzyme 1 antibody (IRE1α, phospho S724, ab48187), rabbit polyclonal anti-NAD(P)H:quinone oxidoreductase antibody (NQO1, ab34173) were obtained from Abcam (Cambridge, UK). Terminal deoxynucleotidyl transferase, recombinant (rTdT) was obtained from Affymetrix (Santa Clara, CA). AIDS Research and Reference Reagent Program, Division of AIDS, NIAID, NIH supplied antiretroviral reagents. Mouse monoclonal anti-BiP/Grp78 antibody (610978) was obtained from BD Transduction Laboratories (San Jose, CA). Rabbit polyclonal anti-eukaryotic initiation factor 2 alpha antibody (eIF2α, 9722S), and rabbit polyclonal anti-phospho-eukaryotic initiation factor 2 alpha (Ser51) antibody (p-eIF2α, 9721S) were obtained from Cell Signaling Technology (Beverly, MA). Chemicon International (Temecula, CA) provided mouse monoclonal anti-cyclic-nucleotide-3′phosphodiesterase antibody (CNPase, MAB326R) and mouse monoclonal anti-glyceraldehyde 3-phosphate dehydrogenase antibody (GAPDH, MAB374). Covance Laboratories (Conshohocken, PA) provided mouse monoclonal anti-MBP (SMI-99). Enzo Life Sciences (Plymouth Meeting, PA) provided rabbit polyclonal anti-heme oxygenase-1 antibody (HO-1, SPA-896). B27 supplement, 4%-12% Bis-Tris gradient gels, CAS-block, dihydroethidium (DHE), Dulbecco's Modified Eagle's Medium (DMEM), DMEM/F12, deoxyribonuclease 1 (DNase), Ham's F12, L-glutamine, Hank's Balanced Salt Solution, rabbit polyclonal anti-small/large myelin-associated glycoprotein (MAG) antibody, neurobasal medium, and penicillin/streptomycin were from Life Technologies (Carlsbad, CA). Rhodamine-conjugated goat anti-mouse IgM, FITC-conjugated goat anti-mouse IgG3, Rhodamine-conjugated goat anti-rat IgG, FITC-conjugated goat anti-rat IgG, Rhodamine-conjugated streptavidin. LiCOR (Lincoln, NE): Odyssey goat anti-mouse IRdye 800CW, goat anti-mouse IRdye 680RD, goat anti-rat IRdye 800CW, goat anti-rat IRdye 680RD, goat anti-rabbit IRdye 800CW, goat anti-rabbit IRdye 680RD were from Jackson Immunoresearch Laboratories (West Grove, PA). Peprotech (Rocky Hill, NJ) provided neurotrophin-3. Poly-D-lysine was from Peptide International. Rabbit polyclonal anti-activating transcription factor 6 β antibody (ATF6β, 15794-1-AP)

Author Manuscript Author Manuscript Author Manuscript Author Manuscript

was from Proteintech (Chicago, IL). R&D Systems (Minneapolis, MN) was the source of basic fibroblast growth factor (bFGF), and platelet-derived growth factor-AA (PDGF-AA). Roche Diagnostics (Basel, Switzerland) supplied biotin-16-dUTP. Mouse monoclonal anti-α-tubulin antibody (T5168), biotin, dimethyl sulfoxide (DMSO), fast green FCF, insulin, monomethyl fumarate (MMF), TRITC-conjugated phalloidin, progesterone, protease inhibitor cocktail, putrescine, sodium cacodylate, selenium, tert-Butyl hydroperoxide (tBHP), thyroxine (T4), transferrin were from Sigma (St. Louis, MO). Restore Western Blot Stripping Buffer was from Thermo Fisher Scientific (Waltham, MA). Vectashield with 4′,6-diamidino-2-phenylindole (DAPI) was from Vector Laboratories (Burlingame, CA).

Additional antibodies were anti-A2B5 mouse hybridoma supernatant (ATCC [35]), anti-galactocerebroside mouse hybridoma supernatant (GalC H8H9, [36]), anti-myelin oligodendrocyte glycoprotein (MOG) (37), anti-MBP rat hybridoma supernatant (gift of Virginia Lee, University of Pennsylvania, Philadelphia, PA), anti-proteolipid protein rat hybridoma (AA3, gift of Dr. Alex Gow, Wayne State University, Detroit, MI).

Primary Cortical Oligodendrocyte Cultures

All experiments were performed in accordance with the guidelines set forth by The Children's Hospital of Philadelphia and The University of Pennsylvania Institutional Animal Care and Use Committees. Primary mouse oligodendrocyte precursor cell (OPC) cultures were isolated from postnatal day 1 CD1 pups obtained from Charles River Laboratories, with modifications from previously described protocols (34). Briefly, cortical cell suspensions isolated from mouse pups using standard protocols were plated on poly-D-lysine coated T-75 flasks in Neurobasal medium with B27 supplement at 37°C with 5% CO_2. After 24 hours, cultures were switched to growth medium consisting of Neurobasal medium with B27 which contained 10 ng/ml bFGF, 2 ng/ml PDGF-AA, and 1 ng/ml neurotrophin-3. Within 7 days, confluent cells were purified to 90%-95% OPCs and 5%-15% astrocytes using a gentle wash-down procedure (38), and sub-cultured onto poly-lysine-coated flasks, coverslips, or Petri dishes. For differentiation experiments, growth medium was replaced with differentiation medium, consisting of 50% DMEM, 50% Ham's F12, Pen/Strep and 2 mM glutamine with 50 μg/ml transferrin, 5 μg/ml putrescine, 3 ng/ml progesterone, 2.6 ng/ml selenium, 12.5 μg/ml insulin, 0.4 μg/ml T4, 0.3% glucose, and 10 ng/ml biotin (38).

Immunofluorescence

Cells on coverslips were processed for detection of specific antigens as previously described (34, 39). Prior to fixation, live cells were labeled for cell surface marker detection using anti-A2B5 (mouse hybridoma supernatant, undiluted), and anti-GalC (mouse hybridoma supernatant, undiluted). For detection of internal antigens following acid alcohol fixation and permeabilization, antibodies used were anti-MBP (rat hybridoma supernatant, 1:2 dilution) or anti-proteolipid protein (PLP) (rat hybridoma supernatant, 1:2 dilution). Secondary antibodies used at a 1:100 dilution were Rhodamine- or Fluorescein-conjugated. Vectashield with DAPI was used to mount coverslips, and to stain all nuclei. Antigen-positive and DAPI-positive cells were counted in 10 fields in each of 3 to 4 coverslips from at least 3 biologically separate preparations of cells using a Leica DM6000B fluorescence

Author Manuscript Author Manuscript Author Manuscript Author Manuscript

microscope at 40x magnification. A total of approximately 2000 cells were counted per condition. The chosen and accepted standard method for quantification of differentiation determines the number of cells progressing through various stages using well-defined stage-specific markers (38, 40, 41). For phalloidin staining, cell surface markers were stained as above. Next, cells were fixed with 4% paraformaldehyde for 8 minutes, washed with phosphate buffered saline (PBS), solubilized with 0.5% Triton X-100 in PBS, and blocked for 30 minutes with a 1:1 dilution of 100 mg/ml BSA and CAS-block. Cells were then incubated with TRITC-conjugated phalloidin at a final concentration of 500 nM for 2 hours. Cells were mounted and visualized as described above. To assess cells committed to apoptotic cell death, a TUNEL staining protocol adapted from that of Gavrieli et al was utilized (42). Cells were fixed with ice-cold acetone for 10 minutes, washed with PBS, and solubilized with 0.5% Triton X-100 in PBS for 15 minutes. Positive control coverslips were generated during this period by incubating in DN buffer (30 mM Trizma base pH 7.2, 140 mM Na cacodylate, 4 mM MgCl, and 0.1 mM DTT) for 2 minutes, followed by DNase (1:200) in DN buffer for 10 minutes. All coverslips were washed with PBS then placed in TDT buffer for 2 minutes (30 mM Trizma base pH 7.2, 140 mM Na cacodylate, 1 mM CoCl). Cells were incubated for 1 hour with TdT and biotin-UTP in TDT buffer (8 μL of each in 1mL TDT buffer). Following a subsequent PBS wash, cells were placed in TB buffer for 15 minutes (300 mM NaCl, 30 mM sodium citrate) and then a 2% BSA solution for 30 minutes. Finally cells were incubated with Rhodamine-conjugated streptavidin for 20 minutes prior to a final PBS wash and mounting on slides with Vectashield containing DAPI. Visualization and counting were performed as described above.

Jugular Vein Antiretroviral Administration Mouse Model

Surgical procedures were performed with the approval of the Institutional Animal Care and Use Committee of the University of Pennsylvania. Adult male C57BL/6 mice were catheterized via jugular vein, as described previously (43, 44). Briefly, mice were anesthetized prior to surgery with 80 mg/kg ketamine and 12 mg/kg xylazine. An indwelling silastic catheter (Strategic Applications, Inc.) was placed into the right jugular vein and sutured in place. The catheter was connected to a mesh platform that was subcutaneously placed on the animals back and sutured in place. Catheters were flushed daily with 0.1 ml of the antibiotic Timentin dissolved in heparinized saline (0.93 mg/ml). Treatment regimens were composed of Vehicle (DMSO) or Ritonavir (20 mg/kg), administered twice daily for 14 days by continuous intravenous injection (Vehicle n = 6, Ritonavir n = 7). This drug dose was based on previously published pharmacokinetic studies (45–47). At time of euthanasia, catheter patency was verified by response to pre-euthanasia sedation (80 mg/kg ketamine and 12 mg/kg xylazine). Brains were removed, the frontal cortex, cerebellum, and hippocampi were dissected on ice; tissue samples were stored at −80°C until immunoblot analyses were performed.

Human Subjects

For immunoblotting analyses, samples from a cohort of individuals were obtained from the National NeuroAIDS Tissue Consortium (NNTC) and the Texas NeuroAIDS Research Center. The cohort encompasses 20 HIV-negative, 20 HIV-positive cART-naïve, and 20 HIV-positive cART-medicated for greater than 12 months (HIV-positive/ART) cases. Six

Author Manuscript Author Manuscript Author Manuscript Author Manuscript

HIV-positive cART-naïve and 14 HIV-positive cART-medicated subjects had clinically diagnosed HAND. The pathological diagnosis of HIV encephalitis was established in 6 HIV-positive cART-naïve and 1 HIV-positive cART-medicated patients. Diagnosis of HAND by neuropsychological assessment was based on the results from the NNTC neurocognitive test panel guided by Frascati Criteria, which entails evaluation of 7 domains of cognitive functioning at 6-month intervals prior to death (48). NNTC site pathologists rendered nosological diagnoses of HIVE according to established criteria (49). Evaluation of regimen history determined that 85% of cART-medicated patients were PI-experienced and 100% were NRTI-experienced. Table 1 contains complete cohort demographics and clinical data.

The human studies were conducted in accordance with human subject protection protocols, with written consent obtained at 4 collections sites within the USA. The following institutions maintained the IRBs set forth to provide oversight for the protection of human subjects: 1) The University of Texas Medical Branch Office of Research Subject Protections (Galveston, TX); 2) Mount Sinai Medical Center Program for the Protection of Human Subjects (New York, NY); 3) University of California (San Diego, CA); and 4) University of California Los Angeles, Office of the Human Research Protection Program (Los Angeles, CA).

Immunoblotting

Whole cell extracts of primary mouse oligodendrocyte cultures were prepared with ice-cold cell lysis buffer (50 mM Tris pH 7.5, 120 mM NaCl, 0.5% NP-40, 10 mM EDTA, 0.5 mM Na_3VO_4, and 1:100 protease inhibitor cocktail), followed by centrifugation at 14,000 rpm at 4°C for 30 minutes. Whole cell extracts of mouse and human tissue samples were prepared by homogenization of 100 mg dissected frontal cortex tissue in ice-cold tissue extraction buffer (50 mM Tris pH 7.5, 0.5 M NaCl, 1% NP-40, 1% SDS, 2 mM EDTA, 2 mM EGTA, 5 mM NaF, 0.4 mM Na_3VO_4, 1 mM DTT and 1:100 protease inhibitor cocktail), followed by centrifugation at 14,000 rpm at 4° C for 30 minutes. Protein concentrations of collected supernatants were determined by the Bradford Method. Ten to 25 μg of protein was loaded into each lane of 4%-12% Bis-Tris gradient gels for separation. For detection of PLP, gels were run under non-reducing conditions due to antibody specificity. A broad-spectrum molecular weight ladder was run on each gel. Following separation, proteins were transferred onto Millipore Immobilon-FL membranes, and blocked in PBS with 0.1% Tween-20 (PBST) and 5% milk for 20 minutes at 4°C. Membranes were incubated overnight at 4°C with primary antibodies in PBST + 5% milk. Primary antibodies to the following antigens were used: MBP (SMI-99, 1:1000 dilution), PLP (1:1000 dilution), MAG (1:500 dilution), CNPase (1:1000 dilution), HO-1 (1:1000 dilution), NQO1 (1:1000 dilution), BiP (1:1000 dilution), phospho-eIF2α (1:1000), total eIF2α (1:1000), phospho-IRE1α (1:1000), total IRE1α (1:1000), and ATF6β (1:1000). Membranes were washed with PBST, re-blocked for 20 minutes in PBST+ 5% milk, and incubated with corresponding antigen-specific fluorescent probe-conjugated secondary antibodies (1:10,000 dilution) in PBST + 5% milk. Membranes were visualized using an Odyssey Infrared Imaging System (LiCOR). Loading controls were obtained by reblotting for GAPDH (1:1000 dilution), α-tubulin (1:1000 dilution), or FastGreen FCF. To obtain ratios of phosphorylated to total

Author Manuscript Author Manuscript Author Manuscript Author Manuscript

protein levels for eIF2α and IRE1α, first phosphorylated proteins were detected. Following visualization, membranes were stripped using Restore Western Blot Stripping Buffer and re-examined using the Odyssey to ensure all detectable first-round antibodies were removed. Membranes were then re-blocked and incubated with the corresponding primary antibodies for total eIF2α or IRE1α. Bands of interest were specified to determine pixel intensities for each treatment using the NIH ImageJ program (V 1.36b, Bethesda, MD), and the band intensities were normalized to loading controls to ensure equal loading. Proteins of interest were quantified by analyzing bands corresponding to the appropriate molecular weight reported by the manufacturers and observed in our previous studies. In mouse and human brain tissue in which myelin proteins are found in high abundance, MBP and MAG present as doublets, which were evaluated simultaneously and quantified. FastGreen staining was used for samples from tissue to ensure protein integrity as well as equal loading. To quantify FastGreen densitometry, a horizontal section of the membrane spanning a broad molecular weight range was scanned together, and overall intensity was determined for each lane. This method allows for normalization across lanes within gels without bias towards a single representative protein loading control. Due to large sample size in the human studies, a standard combined sample was run on each gel, and values were then normalized across gels.

Measurement of reactive oxygen species (ROS)

The superoxide indicator DHE was used to detect the presence of ROS in vitro. Fifteen minutes prior to conclusion of treatments, 3 μM DHE was added to the culture medium. Oxidation of DHE to ethidium allows for ethidium intercalation with nuclear DNA, emitting a quantifiable red fluorescence (50). Cells were washed with F12 medium and fixed with 4% paraformaldehyde at room temperature for 8 minutes. The coverslips were then washed with F12 medium, mounted on slides with DAPI-containing Vectashield, and visualized using fluorescent microscopy, as described above. The oxidant tert-Butyl hydroperoxide (tBHP, 2.5 μM) was used as a positive indicator of ROS in culture. Post-acquisition analysis was performed using MetaMorph 6.0 software (Molecular Devices, Sunnyvale, CA) to determine the fluorescence intensity of nuclear intercalated DHE normalized to the area of DAPI signal.

Quantitative Reverse Transcription Polymerase Chain Reaction

The expression of HO-1, NQO1, spliced X-box binding protein-1 (XBP-1), total XBP-1, BiP, C/EBP homologous protein (CHOP), IRE1α, ATF6β and activating transcription factor 4 (ATF4) mRNA in oligodendrocyte cultures were quantified by quantitative reverse transcription polymerase chain reaction (RT-PCR). OPC cultures were grown on 100-mm dishes and harvested after treatment with specified antiretrovirals for 6 hours. RNA was extracted with Trizol, and 5 μg of RNA was converted to cDNA by the Invitrogen Superscript First-strand kit. Quantitative PCR was performed using Power SYBR Green, as previously described (51–52). Samples were measured in triplicate for each experiment from 3 biological replicates (n = 3). Data were normalized using protein kinase gene 1, and analyzed according to the ΔΔCT method. Primer pairs obtained from Integrated DNA Technologies (Coralville, IA), for each gene are listed in Table 2.

Author Manuscript Author Manuscript Author Manuscript Author Manuscript

Statistical Analysis

All data were analyzed by Prism 5.0 software (GraphPad Software, San Diego, CA). Values are expressed as mean ± SE. All statistical tests compared Zidovudine (AZT) to Untreated as it was dissolved in water, and Lopinavir and Ritonavir to the Vehicle (DMSO) in which they were resuspended. Following differentiation, untreated and vehicle-treated cultures do not statistically differ in the number of cells staining with anti-GalC, which marks immature oligodendrocytes, or MBP and PLP, which mark mature oligodendrocytes (data not shown). One-way ANOVA with post-hoc Newman-Keuls multiple comparison test, one-way ANOVA with post-hoc Dunnett's multiple comparison test or Student t-test were performed where indicated. For comparison of specific treatment groups at 2 time points, one-way ANOVA with post-hoc Bonferroni correction was performed. Values of $p < 0.05$ were considered significant for all analyses.

RESULTS

HIV Protease Inhibitors Prevent Oligodendrocyte Differentiation

The potential impacts of antiretroviral compounds on oligodendrocyte survival, maturation, or myelination have not been determined to date. We chose to test 3 widely prescribed antiretroviral drugs: Zidovudine (AZT), a nucleoside/nucleotide reverse-transcriptase inhibitor (NRTI), and Ritonavir and Lopinavir, two protease inhibitors (PI). We based our range of antiretroviral doses on previously reported plasma and cerebrospinal fluid (CSF) levels in humans, as measurements from human brain parenchyma have not been performed (53–57). Many antiretrovirals are thought to have limited CNS penetrance due to pharmacological properties that impair their transport across the blood brain barrier and promote active exclusion through efflux transporters (58–60). However, there is extensive evidence of HIV-mediated disruption of the blood brain barrier resulting in increased entry of normally excluded small molecules and serum proteins (61–63). In addition to HIV-mediated effects, even in the absence of virus, CNS accessibility is not necessarily as restricted as anticipated, as brain entry can be facilitated if the drugs are given in combination (64). Importantly, animal studies predict that parenchymal concentrations reach levels equal to, or greater than those found in the CSF, suggesting that concentrations attained in the human brain may be higher than current clinical estimates (65, 66).

We first determined the dose-dependent effects of these compounds on differentiation utilizing our previously described paradigm (34). Primary mouse oligodendrocyte precursor cells (OPCs) were purified and grown in the presence of bFGF, PDGF-AA, and neurotrophin-3 to 75% confluence, at which time growth factors were removed and thyroid hormone was added to initiate differentiation, allowing OPCs to progress first to immature then mature oligodendrocytes. OPCs were allowed to differentiate for 72 hours in the presence of Vehicle (DMSO) or the antiretrovirals tested: AZT (1 μM, 10 μM, or 25 μM), Ritonavir (100 nM, 1 μM, or 3 μM), or Lopinavir (150 nM, 1.5 μM, or 15 μM). Oligodendrocyte maturation is well defined and regulated; therefore, cellular markers correlating to specific stages of differentiation are commonly used to illustrate lineage progression (40). A2B5 was used as a marker of OPCs, GalC as a marker of immature oligodendrocytes, and MBP or PLP as markers of mature oligodendrocytes.

Author Manuscript Author Manuscript Author Manuscript Author Manuscript

Immunofluorescent staining following treatments revealed that the PIs Ritonavir and Lopinavir but not NRTI AZT resulted in fewer cells expressing differentiation markers, compared with controls. Representative images of oligodendrocytes after 72 hours in differentiation medium demonstrate dose-dependent maturation decreases with PIs (Fig. 1A), with the extent of maturation determined by comparing the percentage of GalC-positive cells and MBP-positive cells across treatments (Fig. 1B, C). Following PI treatment, the number of cells expressing the immature marker GalC after 3 days of differentiation was reduced by 69.43% ± 6.07% for the highest dose of Ritonavir and by 95.63% ± 0.96% with the highest dose of Lopinavir, compared with vehicle controls ($p < 0.001$) (Fig. 1B). Similarly, the number of MBP-positive cells was significantly reduced by 75.14% ± 4.94% with Ritonavir and by 97.62% ± 1.03% with Lopinavir treatments compared with vehicle ($p < 0.001$) (Fig. 1C). In contrast, AZT treatment did not alter the number of GalC-positive or MBP-positive cells, compared with controls (Fig. 1B, C). Quantification of PLP-positive cells mirrored that of MBP-positive cells for all conditions (data not shown).

Changes in the number of cells expressing markers of oligodendrocyte differentiation could be attributed to cell death, altered precursor proliferation, or inhibition of differentiation. To address changes in cell death or OPC proliferation, we determined the number of total cells (DAPI-positive cells) (Fig. 2A) and A2B5-positive OPCs (Fig. 2B) following treatments. AZT, which did not cause a loss of GalC-positive or MBP-positive oligodendrocytes compared to controls, did not lead to a loss of OPCs or total cells at any dose as expected. Interestingly, Ritonavir, at any dose, also did not lead to loss of OPCs or total cell number in culture, suggesting that Ritonavir treatment decreased GalC-positive and MBP-positive oligodendrocytes by inhibition of the differentiation process. In contrast, Lopinavir treatment trended towards a reduction in total cell number at the 1.5 μM dose (81.5% ± 5.52%), and significantly decreased total cell numbers at the 15 μM dose (73.9% ± 6.29% of vehicle total) ($p < 0.05$) (Fig. 2A). A significant reduction between the 1.5 μM and 15 μM concentrations was not observed. Lopinavir did not alter A2B5-positive precursor cell number at any concentration (Fig. 2B). These observed decreases, although significant, are modest compared to the near total loss of GalC-positive and MBP-positive cells with 15 uM Lopinavir treatment. To verify that the dramatic reductions observed in expression of GalC and MBP following Lopinavir treatment were due to inhibition of differentiation and not apoptotic cell death, we assessed whether remaining cells were committed to the apoptotic cell death cascade using the TUNEL assay, which labels double-stranded DNA breaks in extensively damaged cells. Treatment with 15 μM and 1.5 μM concentrations of Lopinavir resulted in negligible TUNEL-positive cells, similar to vehicle treatment (Fig. 2C). Together, these results suggest that Lopinavir inhibits proper oligodendrocyte maturation in a dose-dependent manner. The modest reductions in GalC-positive and MBP-positive cells observed at 1.5 μM (57.0% ± 12.43% and 56.7% ± 12.72% of control differentiation levels) plummeted to 4.37% ± 0.96% and 2.38% ± 1.03%, respectively, at 15 μM without activation of the apoptotic cascade or a significant reduction in cell number between these 2 concentrations.

Author Manuscript Author Manuscript Author Manuscript Author Manuscript

Lopinavir Reduces the Expression of Myelin Proteins

Given that PI-treated cultures contained fewer GalC-positive, MBP-positive and PLP-positive cells (as compared with vehicle) by immunofluorescence, we next determined whether this effect resulted from decreased protein levels. The cultures were treated as described above for 72 hours, and protein lysates were prepared for immunoblot analysis. The highest dose of Lopinavir (15 μM) led to a significant decrease in MBP levels when compared with vehicle ($p < 0.01$) (Fig. 3C). In contrast, neither AZT nor Ritonavir significantly altered MBP expression levels (Fig. 3A, B). Additionally, PLP and CNPase, 2 other major myelin proteins, were also decreased in 15 μM Lopinavir-treated cells compared with controls, whereas no change in either protein was observed following high dose (25 μM) Azt or (3 μM) Ritonavir treatments (Fig. 3D, E). This immunoblotting analysis of Lopinavir treated cells parallels that of the immunofluorescence results in Figure 1, with dramatic reductions in protein markers of maturation observed between the 1.5 μM and 15 μM concentrations of Lopinavir (Fig. 2A). Intriguingly, all doses of Ritonavir and the intermediate dose of Lopinavir (1.5 μM) decreased the number of GalC-positive and MBP-positive cells by immunofluorescence, but not myelin protein levels by immunoblot.

PI-Mediated Reduction of Differentiation is Reversible

Our observation that at low doses of PIs there were significantly fewer mature oligodendrocytes, despite unchanged levels of myelin proteins prompted us to determine whether oligodendrocyte processes were elaborated but myelin proteins were not being properly localized. Therefore, we utilized phalloidin staining to visualize actin microfilaments. Cells were treated with vehicle, 3 μM Ritonavir, or 15 μM Lopinavir and allowed to mature for 72 hours, followed by phalloidin staining. As shown in the representative images of Figure 4A, cells maintained normal differentiated geometry and process extension after treatment; however, the immature oligodendrocyte stage marker GalC did not appear to correctly localize to the cell surface.

To determine if the effects of the PIs were permanent, or if cells were still capable of proper myelin protein production and localization, we differentiated OPCs in the presence of 3 μM Ritonavir or 15 μM Lopinavir and allowed 72 hours for maturation. At this time, a subset of cultures was switched into fresh differentiation medium lacking further treatment for an additional 24 hours. Cultures that underwent a drug washout period were analyzed for markers of oligodendrocyte differentiation and compared with the cultures that did not undergo drug washout but were exposed to PI treatments for 72 hours. As we have shown in Figure 1, whereas 72-hour treatment with 3 μM Ritonavir or 15 μM Lopinavir resulted in fewer GalC-positive cells compared with vehicle, this effect was completely reversed after the removal of both PIs (Fig. 4B). Similarly, drug washout for 24 hours resulted in the reversal of the deficit in MBP levels following treatment with 15 μM Lopinavir (0.28 ± 0.12 fold of control levels, $p < 0.05$), as detected by immunoblotting (Fig. 4C). In 15 μM Lopinavir treated cultures, the rapid restoration of maturation to vehicle-treated levels following drug washout further corroborates the findings from Figures 1–3, which together substantiate that cell death did not cause the original reduction in myelin proteins and cell surface markers of differentiation following Lopinavir treatment.

Author Manuscript Author Manuscript Author Manuscript Author Manuscript

Antiretroviral Drugs Induce Oxidative Stress

Previous work from our laboratory has shown that oxidative stress is capable of halting oligodendrocyte differentiation (51, 67). We have also demonstrated in primary neuroglial cultures that antiretroviral compounds (PIs and NRTIs) evoke the generation of ROS (32). In light of this, we postulated that oxidative stress could be the instigating factor for altered differentiation in the presence of Ritonavir and Lopinavir. OPCs were exposed to AZT, Ritonavir, and Lopinavir for 30 minutes, 1 hour, 2 hours, 6 hours, 12 hours, or 24 hours at the doses used in previous experiments, followed by staining with DHE as an indicator of ROS. This method is a read-out for cellular ROS levels, as oxidation of DHE to ethidium allows for ethidium intercalation with DNA, emitting a quantifiable red fluorescence that overlaps with DAPI area (50). Tert-butyl hydroperoxide (tBHP, 2.5 μM) treatment was used as positive indicator of ROS generation for each time point. Following the time course outlined above, we found that Ritonavir produced a dose-dependent, rapid and robust accumulation of ROS by 1 hour (1756% ± 360.8% compared with vehicle, $p < 0.001$), while AZT produced a more modest effect, which was not observed until 2 hours post-treatment (505% ± 80.4% compared with control, $p < 0.001$) (Fig. 5). Interestingly, Lopinavir did not produce detectable ROS levels at any time point up to 24 hours (not shown).

The Endogenous Antioxidant Response Is Not Activated With Antiretroviral Drugs in Developing OPCs

Robust ROS were rapidly detectable following Ritonavir and AZT treatments. The typical cellular response to such an imbalance in redox homeostasis is activation of the endogenous antioxidant response (EAR) (68). Therefore, we investigated whether exposure of antiretroviral compounds to developing oligodendrocytes activated this cellular stress-signaling pathway. OPCs were treated with the highest dose of each antiretroviral at the time of differentiation. Then, mRNA or protein was extracted 6 or 16 hours later, respectively. The analysis of principle cellular targets of the EAR: heme oxygenase-1 (HO-1) and NAD(P)H:quinone oxidoreductase (NQO1), revealed no changes in mRNA levels after 6 hours of treatment with AZT. Surprisingly, Lopinavir led to a decrease in HO-1 mRNA levels to 0.654 fold compared with vehicle, with a range between 0.331 and 1.294 fold ($p < 0.001$). In contrast, NQO1 levels were significantly increased with both Ritonavir to 1.716 fold (1.474–2.00 fold range, $p = 0.015$) and Lopinavir to 1.272 fold (0.554–2.921 fold range, $p < 0.001$) (Table 3). The incremental changes in NQO1 in our treatments, as compared with the robust increases normally seen with EAR activation with classical pathway inducers suggest that the response may not be functionally significant (Table 3). Consistent with this interpretation, immunoblotting for HO-1 and NQO1 showed no alterations in protein levels following 16 hours of treatment with any of the compounds tested (Fig. 6A, B).

Effective Reduction of ROS Does Not Rescue Maturation Defects

Robust oxidative stress was evident following treatment with Ritonavir, yet the EAR was not activated following treatment with any of the antiretroviral drugs tested. Therefore, we sought to determine if decreasing the accumulation of ROS would rescue the observed differentiation defects. To do this, we utilized the fumaric acid ester monomethyl fumarate (MMF). MMF is the active metabolite of dimethyl fumarate, which is now approved for

Author Manuscript Author Manuscript Author Manuscript Author Manuscript

treatment of multiple sclerosis (69, 70). Importantly, we have previously shown that MMF successfully ameliorates ROS accumulation and antiretroviral-induced toxicity in neuroglial cell cultures (32). To determine whether MMF was effective at reducing ROS accumulation triggered by antiretrovirals in oligodendrocyte cultures, OPCs were pre-treated with 10 μM MMF for 6 hours, followed by supplementation with MMF and/or treated with 25 μM AZT or 3 μM Ritonavir for 2 hours or 15 μM Lopinavir for 6 hours. DHE staining revealed that MMF pre-treatment significantly attenuated ROS accumulation after AZT and Ritonavir treatments (Fig. 7A). As we previously established, Lopinavir did not induce ROS at 6 hours, and MMF had no effect on endogenously detectable ROS levels (Fig. 7A). We next assessed if reducing oxidative stress by attenuating ROS accumulation by MMF would increase the number of mature oligodendrocytes in the presence of PIs. OPCs were pre-treated with MMF for 24 hours prior to switching to differentiation medium, and were treated with 3 μM Ritonavir or 15 μM Lopinavir. MMF was replenished at the time of PI treatment and again every 24 hours. After 72 hours in differentiation medium, cells were stained for GalC and compared with vehicle or cells incubated with MMF without PIs. There was no difference between the number of GalC-positive cells in cultures treated with Ritonavir + MMF or Lopinavir + MMF (Ritonavir 35.2% ± 0.77%, Lopinavir 36.4% ± 18.2% of vehicle) and those exposed to Ritonavir or Lopinavir alone (Ritonavir 29.9% ± 5.90%, Lopinavir 19.9% ± 14.5%) (Fig. 7B). Thus, MMF decreased oxidative stress but did not improve oligodendrocyte differentiation.

The Unfolded Protein Response Is Not Triggered By Antiretroviral Drugs in Maturing Oligodendrocytes

We and others have demonstrated that antiretroviral drugs induce the unfolded protein response (UPR) in neuroglial and somatic cell types (Gannon and Jordan-Sciutto, personal communication) (71, 72). It has also been well documented that the UPR plays an important role in a variety of demyelinating disorders (73). This complex signaling pathway is modulated by the actions of 3 branches, PKR-like ER kinase (PERK), inositol-requiring enzyme 1 (IRE1), and activating transcription factor 6 (ATF6), all of which complex with ER-resident chaperone protein binding immunoglobulin protein ((BiP)/GRP78) in the absence of ER stress (74). Activation of these pathways leads to attenuation of global protein translational in conjunction with selective upregulation of pro-survival proteins (74–76).

Therefore, we analyzed whether the UPR was activated in OPCs treated with antiretroviral drugs for 6 or 16 hours by assessing mRNA and protein levels of markers of UPR activation. Upon disruption of endoplasmic reticulum homeostasis and activation of the UPR, XBP-1 mRNA is spliced to promote the production of the active XBP-1 protein (78, 79). The relative ratio between spliced and total XBP-1 mRNA is an accepted standard for UPR activation (78, 79). The analysis of this ratio revealed no increases in XBP-1 mRNA splicing in antiretroviral-treated cells at 6 hours, suggesting that UPR activation did not occur upon treatment of OPCs with these drugs (Table 4). Whereas Lopinavir treatment led to a significant decrease in XBP-1 mRNA splicing (0.398-fold as compared with vehicle, with a range of 0.297–0.534-fold [$p < 0.001$]) (Table 4), this effect is negligible compared with biologically relevant changes, and does not correspond to the robust increases in the ratio of

Author Manuscript Author Manuscript Author Manuscript Author Manuscript

spliced-to-total XBP-1 mRNA, which would indicate UPR activation. Additional genes targeted by the UPR pathway were also examined by this method. No significant alterations in transcript levels were noted for CHOP, BiP, ATF6, or ATF4 with any antiretroviral tested (Table 4). IRE1α was not altered with Azt or Ritonavir, but was highly upregulated following Lopinavir treatment (8.664-fold compared with vehicle, with a range of 8.532–8.797-fold. Binding immunoglobulin protein (BiP) served as an indicator of UPR activation at the protein level. As the primary sensor of endoplasmic reticulum stress, its cellular levels are tightly regulated by transcription, translation, and selective stabilization during stress conditions (80). Additionally, BiP is known to be upregulated in oligodendrocytes under conditions promoting UPR activation (81). Immunoblotting for BiP protein showed no difference between PI-treated and vehicle cultures (Fig. 8A). To examine the individual arms of the UPR further, Western blotting was performed for post-translational modifications of representative proteins. As eIF2a phosphorylation was not increased following 16 hours of treatment with any antiretroviral, the PERK pathway is likely not involved at this time point (Fig. 8B). ATF6β cleavage was also not observed, suggesting these antiretrovirals do not modulate ATF6-mediated transcriptional activity (Fig. 8C). Finally, despite a significant increase in IRE1α mRNA observed by RT-PCR following Lopinavir treatment, total protein IRE1α protein level was not increased in this condition compared to vehicle (Fig. 8D). More importantly, activation of the IRE1α branch of the UPR is dependent on protein dimerization facilitated by phosphorylation status. IRE1α phosphorylation status was not increased with Lopinavir or any antiretroviral condition (Fig. 8E). Functional activation of the IRE1α pathway arm leads to the splicing event of XBP1 (74–76). Rather than increasing, we observed that XBP1 splicing was significantly decreased following Lopinavir treatment, suggesting potential IRE1 pathway suppression, complete with compensatory increase of regulator IRE1α transcription as was also observed by RT-PCR (Table 4). In summary, these findings suggest that neither the EAR nor the UPR are activated in OPCs by any of the antiretrovirals tested during the timeframe that was previously determined to induce responses within these pathways neuroglial culture. Thus, we do not currently ascribe the observed negative maturation effects to actions of either of these pathways.

Myelin Protein Expression In Vivo Is Reduced After Treatment With a Ritonavir Regimen

After investigating how antiretrovirals altered oligodendrocyte maturation in vitro, we asked whether these compounds also had detrimental effects to established myelin in vivo. To this end, we examined the effects of a repeated/chronic antiretroviral exposure. We administered Ritonavir or vehicle intravenously to adult male mice through implanted jugular vein catheters over a 2-week period, according to the same protocol followed in our previous studies (32, 44). Recommendations for treatment regimens are constantly changing to improve patient outcomes while reducing adverse effects, as well as incorporating new drug classes and next-generation therapeutics. For our purposes, Ritonavir was chosen as a representative antiretroviral compound for our in vivo study. Ritonavir is globally used clinically as a boost for other antiretrovirals to increase bioavailability because it is a potent inhibitor of cytochrome P450, which metabolizes these compounds (82). Increased bioavailability of co-administered compounds with high CNS penetrance likely leads to higher brain levels of these compounds (64). Additionally, Ritonavir-boosted regimens are

Author Manuscript Author Manuscript Author Manuscript Author Manuscript

still commonly prescribed in resource-limited settings as first-line treatment, making it globally among the most-prescribed treatment options (83). The dose of Ritonavir was based on previously published pharmacokinetic studies (45–47). The animals showed no signs of distress or gross phenotypic alterations over the course of treatment. To determine the effects of Ritonavir on established myelin, myelin protein levels were assessed by immunoblotting cellular lysates prepared from frontal cortex. In addition to MBP, other components of mature myelin were also evaluated in vivo. We observed that protein levels of MOG and CNPase were significantly decreased with Ritonavir compared with vehicle treatment ($p < 0.05$), whereas MBP, MAG, and PLP levels were not significantly altered (Fig. 9).

Myelin Protein Expression in Humans Is Altered by HIV- and Antiretroviral Treatment Status

To address potential translational relevance of our observations, we examined prefrontal cortex autopsy specimens from cohort of HIV-infected patients who had been treated with antiretroviral agents. To date, diffusion tensor and magnetic resonance imaging studies and a single transcriptome study have been performed to examine white matter dysfunction in HIV and HAND patients (17, 19, 20), but changes in postmortem myelin protein levels have not been reported. The cohort contained age-matched HIV-negative, HIV-positive patients who were cART-naïve (HIV-positive), and HIV-positive cART-medicated >12 month individuals (HIV-positive/ART) ($n = 20$ for each group). The HIV-positive cART-naïve group was comprised of 6 individuals with diagnosed HAND, 1 who was neurocognitively normal and 5 with neuropsychological impairments that were potentially due to factors other than HIV infection. Eight of the cases did not undergo a structured antemortem neurocognitive assessment. The HIV-positive cART-medicated >12 month group (HIV-positive/ART) contained 14 individuals with HAND, 2 who were neurocognitively normal and 4 with neuropsychological impairments potentially due to factors other than HIV infection. The full details of their demographics and clinical data are summarized in Table 1. The prefrontal cortex was selected for analysis for the following reasons: 1) this brain region is utilized in performing the functional modalities in which HAND patients display impairments (48); 2) synaptodendritic damage has been previously reported in this region in affected patients (84); and 3) a region of mixed white and grey matter was desired for analysis as is seen in the cortex, so that the overall myelin contribution and relative protein amounts could be assessed. Previous studies have shown that the volume of the corpus callosum is reduced in HIV patients and with antiretroviral treatment. Because this is an extremely myelin-rich environment, however, to observe a quantitative change in immunoblot analysis would require a sizable loss of myelination. For all cases, the myelin proteins MBP, MOG, CNPase, and MAG were examined by immunoblot analysis. When subdivided according to HIV status alone, no significant alterations were noted in the myelin protein levels between uninfected controls and the HIV-positive patients (Fig. 10). However, when the cohort was stratified into categories based on antiretroviral therapy status, CNPase protein was significantly increased in the HIV-positive cART > 12 month (HIV-positive/ART) group vs. the HIV-negative group ($p < 0.01$) (Fig. 11A). Finally, individuals for whom neurocognitive data was not known, who were neurocognitively normal, or who had neuropsychological impairment due to factors other than HIV infection were excluded from

Author Manuscript Author Manuscript Author Manuscript Author Manuscript

analysis to remove potential confounding factors and to allow us to examine only those cases with known HAND diagnosis in relation to cART-medication status. This analysis revealed a significant decrease in MBP protein levels in the HIV-positive/ART group as compared with the HIV-negative ($p < 0.05$) and HIV-positive ($p < 0.05$) groups (Fig. 11B). On the other hand, a significant increase in CNPase protein was observed in the HIV-positive/ART group, compared with the HIV-negative group ($p < 0.001$) (Fig. 11B). These results indicate that HIV infection compounded with the effects of antiretroviral therapy can lead to alterations in myelin protein levels in patients.

DISCUSSION

Despite effective viral suppression through antiretroviral therapy, HIV-Associated Neurocognitive Disorders (HAND) persists in infected individuals and is frequently accompanied by pathologic white matter abnormalities (6, 17, 19). Here, we investigated the effects of antiretrovirals in vitro on oligodendrocyte survival and maturation and in vivo on myelin maintenance in both adult mice and HIV-positive individuals. We have provided novel, compelling evidence that the protease inhibitors Ritonavir and Lopinavir impair both the maturation of oligodendrocyte precursors into myelin-producing cells, and the maintenance of myelin proteins in vivo. Furthermore, human brain specimens demonstrated a reduction in MBP and an increase in CNPase in HAND patients who had been cART-medicated for greater than 1 year, suggesting a loss of myelin integrity yet failure of successful remyelination. These novel observations of the effects of a subset of antiretrovirals on oligodendrocyte development and maintenance may have critical clinical repercussions for both pediatric and adult HIV patients.

Utilizing stage-specific markers, we have shown that PIs Ritonavir and Lopinavir prevent oligodendrocyte maturation in vitro whereas NRTI AZT does not. Interestingly, myelin protein levels as evaluated by immunoblotting remained unchanged under most conditions, except at the highest dose of Lopinavir. During normal maturation, OPCs enter into differentiation and proceed with upregulation of myelin component mRNAs (40). During this progression, cells extend actin filaments to elaborate processes. Most myelin proteins are then translated in the perinuclear endoplasmic reticulum and trafficked through the secretory pathway to be inserted into the forming myelin membrane (85). An exception is MBP, in which mRNA is trafficked to sites proximal to membrane insertion where the protein is then translated on free-ribosomes (85, 86). In that context, our data suggest that treatment with PIs prevents proper membrane insertion of both myelin proteins traversing the secretory network and locally synthesized MBP as we have detected by immunofluorescence; however, in these conditions, protein levels remain unchanged, as determined by immunoblotting. Specifically, even at the highest Ritonavir dose where we observed substantial decreases in maturation by immunofluorescence, we did not detect parallel changes at the protein level. This finding, while unusual, is not unprecedented in oligodendrocytes. Maier et al demonstrated that reduction in cellular cholesterol levels can result in decreased PLP surface expression with minimal reduction at the protein level (87). Along these lines, a recent study also suggested that myelin membrane lipid composition may be altered under two models of demyelination. In this work, MBP surface localization to myelinated processes by immunohistochemistry was diminished, while total MBP levels

Author Manuscript Author Manuscript Author Manuscript Author Manuscript

remained unchanged (88). Additionally, a study investigating the role of mammalian target of rapamycin in oligodendrocyte differentiation observed maintenance of normal myelin protein levels despite a significant reduction in the number of maturing oligodendrocytes (89). Further, we observed that cells treated with either PI adopted properly elaborated mature oligodendrocyte morphology, as evidenced by normal actin cytoskeleton morphology despite reduction in myelin protein expression at the cell surface. The effect of PIs was reversible, as cells proceeded to differentiate rapidly following drug removal, with both cell surface marker expression and myelin protein levels indistinguishable from controls after 24 hours. The accelerated rescue of maturation deficits further suggests that required components are already present within the treated cells, and that these PIs are most probably suppressing maturation on a post-translational level. Drug removal alleviates this blockade, resulting in appropriate protein localization to the myelin membrane.

We observed differences in the effects of Ritonavir and Lopinavir. While both are PIs, their differing chemical structures likely result in disparate cellular uptake, metabolism, and intracellular interactions. In agreement with this notion, other commonly prescribed PIs behave differently within cells of the same lineage. For example, inhibition of differentiation was observed with Nelfinavir and Indinavir, but not Amprenavir in adipocytes (90). Similarly, in CNS-derived astrocytes, Nelfinavir and Indinavir displayed striking differences in ROS production, glutathione export, and toxicity (91). Regardless of the differing subcellular effects that Lopinavir and Ritonavir invoke, it is clear based on our observations that properly functioning myelin would not arise following exposure to either PI even at low concentrations.

Several antiretroviral drugs induce ROS, mitochondrial depolarization and neurotoxicity in mixed neuroglial cultures (32, 33), and we have shown that oxidative stress can hinder the process of oligodendrocyte differentiation (51). While both AZT and Ritonavir induced robust ROS accumulation, Lopinavir did not, even at extended time points. When we assessed whether the EAR, which is triggered by cellular redox imbalance, was activated following antiretroviral exposure, no biologically relevant increases in target gene mRNAs or proteins such as HO-1 or NQO1 were detected (68). Furthermore, scavenging of ROS with the antioxidant compound MMF did not rescue PI-induced decreases in oligodendrocyte differentiation despite previously demonstrated neuroprotection (32). PIs have also been shown to activate the UPR in non-CNS cells, which potently suppresses protein translation while upregulating stress-response proteins (71, 72, 80), but we found no evidence of UPR activation in oligodendrocytes following antiretroviral treatments at 2 time points where such activation was evident in neuroglial cultures (32), although we acknowledge that there may be activation at earlier or later time points. Thus, our data suggest that PIs inhibit oligodendrocyte maturation through an alternate mechanism. An intriguing possibility is whether PIs disrupt the crucially important myelin-lipid balance, which may result in inappropriate organization of myelin components, as previously reported (87, 88, 92, 93). Because PIs have been shown to cause dyslipidemia in patients and in non-CNS cell types (71, 94, 95), this could contribute to the white matter loss seen in HAND patients (17, 19).

Author Manuscript Author Manuscript Author Manuscript Author Manuscript

The effects of antiretrovirals on myelin in vivo using both a mouse model and human autopsy cases also indicate alterations in myelin proteins. In mice, we detected reduced levels of less abundant myelin protein in as little as 14 days of chronic exposure. Levels of the abundant structural myelin components MBP and PLP were not affected in this short-term administration model. Changes in these critical proteins may be unexpected in such a short time frame as gross changes in myelin may be necessary to result in detectable alterations. In our human cohort, we did observe a reduction in MBP in cART-experienced individuals with HAND compared with cART-naïve individuals with HAND, and HIV-negative controls. This finding correlates with a transcriptome analysis of virally controlled patients with HAND, which showed reduction of MBP mRNA (20). The HIV-positive/ART group also displayed a significant increase in the amount of CNPase over both HIV-negative and HIV-positive cART-naïve individuals, regardless of their neurocognitive status. CNPase is the earliest myelin protein to be expressed during maturation (41), and our observation may reflect a remyelination attempt that is prematurely halted, failing to form mature myelin.

Current WHO guidelines urge immediate treatment of all infected children under the age of 5 years, and adults with a CD4 count ≤ 350 cells/mm^3 consist of 2 NRTIs and a non-nucleoside reverse-transcriptase inhibitor (nNRTI). When second-line cART is necessary due to acquired drug resistance, recommended regimens are composed of 2 NRTIs plus a Ritonavir-boosted PI, either Lopinavir or Atazanavir. All infected children under 3 years of age are recommended a Lopinavir/Ritonavir first-line regimen (7). As is clear from these guidelines, PI-based regimens are extensively used in HIV treatment, particularly in children, during a time of critical cortical myelination, which primarily occurs from the postnatal period until late adolescence (24). Neurological complications are common in infected children, with documentation of encephalopathy, progressive multifocal leukoencephalopathy, cerebrovascular events, and emerging neurocognitive deficits leading to developmental delays, motor, cognitive, and behavioral deficits (21–23). Our results showing an effective disruption in myelination following PI exposure may underlie these clinical presentations, and therefore have important ramifications for the future treatment of pediatric HIV infection.

PI-supplemented regimens are generally prescribed to adults as second-line options. However, because lifelong cART adherence is necessary, over the course of regimen alterations most patients will be exposed to a boosted PI. The maintenance and replacement of myelin in the brain is an active and ongoing process, which is critical for proper neuronal functioning and survival (96). Remyelination of neurons in the adult has been well documented, particularly through investigation into pathology and potential treatments for Multiple Sclerosis (97, 98). Additionally, while traditionally viewed as an early life event, active myelin formation in adulthood is required for motor learning (99, 100). We have shown through our mouse model that prolonged PI exposure may lead to reductions in adult cortical myelin proteins. More importantly, human patients with HAND who had been treated with antiretrovirals for at least a year demonstrated a significant reduction in MBP compared with uninfected individuals and HAND patients who were cART-naïve. Therefore, therapeutics that will preserve the capacity for myelin formation and the integrity of existing structures are of vital importance.

Author Manuscript Author Manuscript Author Manuscript Author Manuscript

In summary, this study implicates antiretrovirals as a contributor to HAND pathology and its persistence in virologically suppressed individuals. In human patients, the underlying viral infection complicates analysis of consequences solely due to antiretrovirals. Our observed effects of antiretrovirals in conjunction with the potential contribution of HIV-induced pathogenesis on oligodendrocytes highlight the necessity for strategic drug development for new therapeutics with fewer deleterious side effects. While this study has highlighted the effects of antiretroviral compounds, future work investigating the consequences of HIV infection in the CNS on the oligodendrocyte population are also essential for a more complete understanding of the changes to white matter in HIV-positive patients.

Furthermore, we must consider adjunctive therapies designed not only to alleviate neuronal dysfunction, but also to preserve myelin formation and maintenance by oligodendrocytes. Persistent ROS elevation and oxidative damage are seen in treated HIV-positive individuals (101, 102). HO-1 deficiency has recently been reported in HIV-positive and HAND patients, suggesting inactivity of the EAR pathway (103). Supporting this notion, we have reported that EAR and HO-1 upregulation by the antioxidant MMF was successful in preventing antiretroviral-induced oxidative stress and neuronal toxicity in neuroglial cultures (32). Unfortunately, based on our current findings, while neurons may be initially protected by adjunctive antioxidant therapy, oligodendrocytes would remain vulnerable and neuronal pathology caused by myelin disruption would still persist. Thus, the effects of antiretrovirals on oligodendrocyte maturation and myelin unveiled in this study illuminate the need for greater understanding of viral- and therapy-mediated repercussions to the critically important oligodendroglial cell population in order to attenuate neurocognitive deficits in HIV-positive individuals in the cART era.

Acknowledgments

We would like to thank the laboratory of Michael Robinson at The Children's Hospital of Philadelphia for use of the Odyssey imaging system, and the National NeuroAIDS Tissue Consortium (NNTC) for providing human patient samples for analysis.

References

1. Kaul M, Zheng J, Okamoto S, et al. HIV-1 Infection and AIDS: consequences for the central nervous system. Cell Death Different. 2005; 12:878–92.
2. Ozdener H. Molecular mechanisms of HIV-1 associated neurodegeneration. J Biosci. 2005; 30:391–405. [PubMed: 16052077]
3. Heaton R, Clifford DB, Franklin DR, et al. HIV-associated neurocognitive disorders persist in the era of potent antiretroviral therapy. Neurology. 2010; 75:2087–96. [PubMed: 21135382]
4. Heaton R, Franklin DR, Ellis RJ, et al. HIV-associated neurocognitive disorders before and during the era of combination antiretroviral therapy: differences in rates, nature, and predictors. J Neurovirol. 2011; 17:3–16. [PubMed: 21174240]
5. McArthur JC, Steiner J, Sacktor N, et al. Human immunodeficiency virus-associated neurocognitive disorders: Mind the gap. Ann Neurol. 2010; 67:699–714. [PubMed: 20517932]
6. Sacktor N, Robertson K. Evolving clinical phenotypes in HIV-associated neurocognitive disorders. Curr Opin HIV AIDS. 2014; 9:517–20. [PubMed: 25203640]
7. World Health Organization. Consolidated guidelines on the use of antiretroviral drugs for treating and preventing HIV infection: recommendations for a public health approach. Jun.2013
8. Anthony I, Ramage SN, Carnie FW, et al. Influence of HAART on HIV-related CNS disease and deuroinflammation. J Neuropathol Exp Neurol. 2005; 64:529–36. [PubMed: 15977645]

Author Manuscript Author Manuscript Author Manuscript Author Manuscript

9. Persidsky Y, Poluektova L. Immune privilege and HIV-1 persistence in the CNS. Immunol Rev. 2006; 213:180–94. [PubMed: 16972904]
10. Wong J, Hezareh M, Gunthard HF, et al. Recovery of replication-competent HIV despite prolonged suppression of plasma viremia. Science. 1997; 278:1291–5. [PubMed: 9360926]
11. Finzi D, Hermankova M, Pierson T, et al. Identification of a reservoir for HIV-1 in patients on highly active antiretroviral therapy. Science. 1997; 278:1295–300. [PubMed: 9360927]
12. Chun T, Stuyver L, Mizell SB, et al. Presence of an inducible HIV-1 latent reservoir during highly active antiretroviral therapy. Proc Natl Acad Sci USA. 1997; 94:13193–7. [PubMed: 9371822]
13. Brew B. Evidence for a change in AIDS dementia complex in the era of highly active antiretroviral therapy and the possibility of new forms of AIDS dementia complex. AIDS. 2004; 18:S75–S8. [PubMed: 15075501]
14. Gray F, Chretien F, Vallat-Decouvelaere AV, et al. The changing pattern of HIV neuropathology in the HAART era. J Neuropathol Exp Neurol. 2003; 62:429–40. [PubMed: 12769183]
15. Tate DF, Conley J, Paul RH, et al. Quantitative diffusion tensor imaging tractography metrics are associated with cognitive performance among HIV-infected patients. Brain Imaging Behav. 2010; 4:68–79. [PubMed: 20503115]
16. Muller-Oehring EM, Schulte T, Rosenbloom MJ, et al. Callosal degradation in HIV-1 infection predicts hierarchical perception: a DTI study. Neuropsychologia. 2010; 48:1133–43. [PubMed: 20018201]
17. Tate DF, Sampat M, Harezlak J, et al. Regional areas and widths of the midsagittal corpus callosum among HIV-infected patients on stable antiretroviral therapies. J Neurovirol. 2011; 17:368–79. [PubMed: 21556960]
18. Ragin AB, Storey P, Cohen BA, et al. Whole brain diffusion tensor imaging in HIV-associated cognitive impairment. AJNR Am J Neuroradiol. 2004; 25:195–200. [PubMed: 14970017]
19. Kelly SG, Taiwo BO, Wu Y, et al. Early suppressive antiretroviral therapy in HIV infection is associated with measurable changes in the corpus callosum. J Neurovirol. 2014; 20:514–20. [PubMed: 24965253]
20. Borjabad A, Morgello S, Chao W, et al. Significant effects of antiretroviral therapy on global gene expression in brain tissues of patients with HIV-1-associated neurocognitive disorders. PLoS Pathog. 2011; 7:e1002213. [PubMed: 21909266]
21. Wilmshurst JM, Burgess J, Hartley P, et al. Specific neurologic complications of human immunodeficiency virus type 1 (HIV-1) infection in children. J Child Neurol. 2006; 21:788–94. [PubMed: 16970887]
22. Wilmshurst JM, Donald KA, Eley B. Update on the key developments of the neurologic complications in children infected with HIV. Curr Opin HIV AIDS. 2014; 9:533–8. [PubMed: 25188807]
23. Crowell CS, Malee KM, Yogev R, et al. Neurologic disease in HIV-infected children and the impact of combination antiretroviral therapy. Rev Med Virol. 2014; 24:316–31. [PubMed: 24806816]
24. Miller DJ, Duka T, Stimpson CD, et al. Prolonged myelination in human neocortical evolution. Proc Natl Acad Sci U S A. 2012; 109:16480–5. [PubMed: 23012402]
25. Edgar JM, Garbern J. The myelinated axon is dependent on the myelinating cell for support and maintenance: molecules involved. J Neurosci Res. 2004; 76:593–8. [PubMed: 15139018]
26. Lappe-Siefke C, Goebbels S, Gravel M, et al. Disruption of Cnp1 uncouples oligodendroglial functions in axonal support and myelination. Nat Genet. 2003; 33:366–74. [PubMed: 12590258]
27. Criste G, Trapp B, Dutta R. Axonal loss in multiple sclerosis: causes and mechanisms. Handb Clin Neurol. 2014; 122:101–13. [PubMed: 24507515]
28. Mighdoll MI, Tao R, Kleinman JE, et al. Myelin, myelin-related disorders, and psychosis. Schizophr Res. 2015; 161:85–93. [PubMed: 25449713]
29. Marra C, Zhao Y, Clifford DB, et al. Impact of combination antiretroviral therapy on cerebrospinal fluid HIV RNA and neurocognitive performance. AIDS. 2009; 23:1359–66. [PubMed: 19424052]
30. Joska JA, Gouse H, Paul RH, et al. Does highly active antiretroviral therapy improve neurocognitive function? A systematic review. J Neurovirol. 2010; 16:101–14. [PubMed: 20345318]

Author Manuscript Author Manuscript Author Manuscript Author Manuscript

31. Kahouadji Y, Dumurgier J, Sellier P, et al. Cognitive function after several years of antiretroviral therapy with stable central nervous system penetration score. HIV Med. 2013; 14:311–5. [PubMed: 23035982]
32. Akay C, Cooper M, Odeleye A, et al. Antiretroviral drugs induce oxidative stress and neuronal damage in the central nervous system. J Neurovirol. 2014; 20:39–53. [PubMed: 24420448]
33. Robertson K, Liner J, Meeker RB. Antiretroviral neurotoxicity. J Neurovirol. 2012
34. See J, Zhang X, Eraydin N, et al. Oligodendrocyte maturation is inhibited by bone morphogenetic protein. Mol Cell Neurosci. 2004; 26:481–92. [PubMed: 15276151]
35. Eisenbarth GS, Walsh FS, Nirenberg M. Monoclonal antibody to a plasma membrane antigen of neurons. Proc Natl Acad Sci U S A. 1979; 76:4913–7. [PubMed: 388422]
36. Ranscht B, Clapshaw PA, Price J, et al. Development of oligodendrocytes and Schwann cells studied with a monoclonal antibody against galactocerebroside. Proc Natl Acad Sci U S A. 1982; 79:2709–13. [PubMed: 7045870]
37. Piddlesden S, Lassmann H, Laffafian I, et al. Antibody-mediated demyelination in experimental allergic encephalomyelitis is independent of complement membrane attack complex formation. Clin Exp Immunol. 1991; 83:245–50. [PubMed: 1993358]
38. Feigenson K, Reid M, See J, et al. Wnt signaling is sufficient to perturb oligodendrocyte maturation. Mol Cell Neurosci. 2009; 42:255–65. [PubMed: 19619658]
39. Grinspan JB, Franceschini B. Platelet-derived growth factor is a survival factor for PSA-NCAM+ oligodendrocyte pre-progenitor cells. J Neurosci Res. 1995; 41:540–51. [PubMed: 7473886]
40. Miller RH. Regulation of oligodendrocyte development in the vertebrate CNS. Prog Neurobiol. 2002; 67:451–67. [PubMed: 12385864]
41. Scherer SS, Braun PE, Grinspan J, et al. Differential regulation of the 2′,3′-cyclic nucleotide 3′-phosphodiesterase gene during oligodendrocyte development. Neuron. 1994; 12:1363–75. [PubMed: 8011341]
42. Gavrieli Y, Sherman Y, Ben-Sasson SA. Identification of programmed cell death in situ via specific labeling of nuclear DNA fragmentation. J Cell Biol. 1992; 119:493–510. [PubMed: 1400587]
43. Thrivikraman KV, Huot RL, Plotsky PM. Jugular vein catheterization for repeated blood sampling in the unrestrained conscious rat. Brain Res Brain Res Protoc. 2002; 10:84–94. [PubMed: 12431707]
44. Briand LA, Lee FS, Blendy JA, et al. Enhanced extinction of cocaine seeking in brain-derived neurotrophic factor Val66Met knock-in mice. Eur J Neurosci. 2012; 35:932–9. [PubMed: 22394056]
45. Pistell PJ, Gupta S, Knight AG, et al. Metabolic and neurologic consequences of chronic lopinavir/ritonavir administration to C57BL/6 mice. Antiviral Res. 2010; 88:334–42. [PubMed: 20970459]
46. du Plooy M, Viljoen M, Rheeders M. Evidence for time-dependent interactions between ritonavir and lopinavir/ritonavir plasma levels following P-glycoprotein inhibition in Sprague-Dawley rats. Biol Pharm Bull. 2011; 34:66–70. [PubMed: 21212519]
47. Kageyama M, Namiki H, Fukushima H, et al. Effect of chronic administration of ritonavir on function of cytochrome P450 3A and P-glycoprotein in rats. Biol Pharm Bull. 2005; 28:130–7. [PubMed: 15635177]
48. Antinori A, Arendt G, Becker JT, et al. Updated research nosology for HIV-associated neurocognitive disorders. Neurology. 2007; 69:1789–99. [PubMed: 17914061]
49. Budka H, Wiley CA, Kleihues P, et al. HIV-associated disease of the nervous system: review of nomenclature and proposal for neuropathology-based terminology. Brain Pathol. 1991; 1:143–52. [PubMed: 1669703]
50. Zhao H, Kalivendi S, Zhang H, et al. Superoxide reacts with hydroethidine but forms a fluorescent product that is distinctly different from ethidium: potential implications in intracellular fluorescence detection of superoxide. Free Radic Biol Med. 2003; 34:1359–68. [PubMed: 12757846]
51. French HM, Reid M, Mamontov P, et al. Oxidative stress disrupts oligodendrocyte maturation. J Neurosci Res. 2009; 87:3076–87. [PubMed: 19479983]

Author Manuscript Author Manuscript Author Manuscript Author Manuscript

52. Feigenson K, Reid M, See J, et al. Canonical Wnt signalling requires the BMP pathway to inhibit oligodendrocyte maturation. ASN Neuro. 2011; 3:e00061. [PubMed: 21599637]
53. Wynn HE, Brundage RC, Fletcher CV. Clinical Implications of CNS penetration of antiretroviral drugs. CNS Drugs. 2002; 16:595–609. [PubMed: 12153332]
54. Cusini A, Vernazza PL, Yerly S, et al. Higher CNS penetration-effectiveness of long-term combination antiretroviral therapy is associated with better HIV-1 viral suppression in cerebrospinal fluid. J Acquir Immune Defic Syndr. 2013; 62:28–35. [PubMed: 23018371]
55. Tiraboschi J, Imaz A, Ferrer E, et al. CSF LPV concentrations and viral load in viral suppressed patients on LPV/r monotherapy given once daily. J Int AIDS Soc. 2014; 17:19587. [PubMed: 25394093]
56. Noor MA, Flint OP, Maa JF, et al. Effects of atazanavir/ritonavir and lopinavir/ritonavir on glucose uptake and insulin sensitivity: demonstrable differences in vitro and clinically. AIDS. 2006; 20:1813–21. [PubMed: 16954722]
57. Decloedt EH, Rosenkranz B, Maartens G, et al. Central nervous system penetration of antiretroviral drugs: pharmacokinetic, pharmacodynamic and pharmacogenomic considerations. Clin Pharmacokinet. 2015; 54:581–98. [PubMed: 25777740]
58. Cysique LA, Brew BJ. Neuropsychological functioning and antiretroviral treatment in HIV/AIDS: a review. Neuropsychol Rev. 2009; 19:169–85. [PubMed: 19424802]
59. McGee B, Smith N, Aweeka F. HIV pharmacology: barriers to the eradication of HIV from the CNS. HIV Clin Trials. 2006; 7:142–53. [PubMed: 16880170]
60. Varatharajan L, Thomas SA. The transport of anti-HIV drugs across blood-CNS interfaces: summary of current knowledge and recommendations for further research. Antiviral Res. 2009; 82:A99–109. [PubMed: 19176219]
61. Toborek M, Lee YW, Flora G, et al. Mechanisms of the blood-brain barrier disruption in HIV-1 infection. Cell Mol Neurobiol. 2005; 25:181–99. [PubMed: 15962513]
62. Wang H, Sun J, Goldstein H. Human immunodeficiency virus type 1 infection increases the in vivo capacity of peripheral monocytes to cross the blood-brain barrier into the brain and the in vivo sensitivity of the blood-brain barrier to disruption by lipopolysaccharide. J Virol. 2008; 82:7591–600. [PubMed: 18508884]
63. Nakagawa S, Castro V, Toborek M. Infection of human pericytes by HIV-1 disrupts the integrity of the blood-brain barrier. J Cell Mol Med. 2012; 16:2950–7. [PubMed: 22947176]
64. Marzolini C, Mueller R, Li-Blatter X, et al. The brain entry of HIV-1 protease inhibitors is facilitated when used in combination. Mol Pharm. 2013; 10:2340–9. [PubMed: 23617680]
65. Anderson PL, Rower JE. Zidovudine and Lamivudine for HIV Infection. Clin Med Rev Ther. 2010; 2:a2004. [PubMed: 20953318]
66. Anthonypillai C, Sanderson RN, Gibbs JE, et al. The distribution of the HIV protease inhibitor, ritonavir, to the brain, cerebrospinal fluid, and choroid plexuses of the guinea pig. J Pharm Exp Ther. 2004; 308:912–20.
67. Reid MV, Murray KA, Marsh ED, et al. Delayed myelination in an intrauterine growth retardation model is mediated by oxidative stress upregulating bone morphogenetic protein 4. J Neuropathol Exp Neurol. 2012; 71:640–53. [PubMed: 22710965]
68. Li W, Kong A. Molecular mechanisms of Nrf2-mediated antioxidant response. Molec Carcinogen. 2009; 48:91–104.
69. Venci JV, Gandhi MA. Dimethyl fumarate (tecfidera): a new oral agent for multiple sclerosis. Ann Pharmacother. 47:1697–702. [PubMed: 24259625]
70. Limmroth V. Multiple sclerosis: oral BG12 for treatment of relapsing-remitting MS. Nat Rev Neurol. 2013; 9:8–10. [PubMed: 23147843]
71. Zhou H, Pandak WM, Lyall V, et al. HIV Protease inhibitors activate the unfolded protein response in macrophages: implication for atherosclerosis and cardiovascular disease. Mol Pharmacol. 2005; 68:690–700. [PubMed: 15976036]
72. Zhou H, Gurley EC, Jarujaron S, et al. HIV protease inhibitors activate the unfolded protein response and disrupt lipid metabolism in primary hepatocytes. Am J Physiol Gastrointest Liver Physiol. 2006; 291:G1071–G80. [PubMed: 16861219]

Author Manuscript Author Manuscript Author Manuscript Author Manuscript

73. Gow A, Wrabetz L. CHOP and the endoplasmic reticulum stress response in myelinating glia. Curr Opin Neurobiol. 2009; 19:505–10. [PubMed: 19744850]
74. Hetz C, Chevet E, Oakes SA. Proteostasis control by the unfolded protein response. Nat Cell Biol. 2015; 17:829–38. [PubMed: 26123108]
75. Bertolotti A, Zhang Y, Henderson LM, et al. Dynamic interaction of BiP and ER stress transducers in the unfolded-protein response. Nat Cell Biol. 2000; 2:326–32. [PubMed: 10854322]
76. Lee J, Ozcan U. Unfolded protein response signaling and metabolic diseases. J Biol Chem. 2014; 289:1203–11. [PubMed: 24324257]
77. Haze K, Yoshida H, Yanagi H, et al. Mammalian transcription factor ATF6 is synthesized as a transmembrane protein and activated by proteolysis in response to endoplasmic reticulum stress. Mol Biol Cell. 1999; 10:3787–99. [PubMed: 10564271]
78. Yoshida H, Matsui T, Yamamoto A, et al. XBP1 mRNA is induced by ATF6 and spliced by IRE1 in response to ER stress to produce a highly active transcription factor. Cell. 2001; 107:881–91. [PubMed: 11779464]
79. Calfon M, Zeng H, Urano F, et al. IRE1 couples endoplasmic reticulum load to secretory capacity by processing the XBP-1 mRNA. Nature. 2002; 415:92–6. [PubMed: 11780124]
80. Brown MK, Naidoo N. The endoplasmic reticulum stress response in aging and age-related diseases. Front Physiol. 2012; 3:263. [PubMed: 22934019]
81. Cortopassi G, Danielson S, Alemi M, et al. Mitochondrial disease activates transcripts of the unfolded protein response and cell cycle and inhibits vesicular secretion and oligodendrocyte-specific transcripts. Mitochondrion. 2006; 6:161–75. [PubMed: 16815102]
82. Moyle G, Back D. Principles and practice of HIV-protease inhibitor pharmacoenhancement. HIV Medicine. 2001; 2:105–13. [PubMed: 11737387]
83. AIDSTAR-One UA; Development USAfI, editor. Summary Table of HIV Treatment Regimens. 2012. http://pdf.usaid.gov/pdf_docs/PA00JV1N.pdf
84. Ellis R, Langford D, Masliah E. HIV and antiretroviral therapy in the brain: neuronal injury and repair. Nat Rev Neurosci. 2007; 8:33–44. [PubMed: 17180161]
85. Colman DR, Kreibich G, Frey AB, et al. Synthesis and incorporation of myelin polypeptides into CNS myelin. J Cell Biol. 1982; 95:598–608. [PubMed: 6183276]
86. Ainger K, Avossa D, Diana AS, et al. Transport and localization elements in myelin basic protein mRNA. J Cell Biol. 1997; 138:1077–87. [PubMed: 9281585]
87. Maier O, De Jonge J, Nomden A, et al. Lovastatin induces the formation of abnormal myelin-like membrane sheets in primary oligodendrocytes. Glia. 2009; 57:402–13. [PubMed: 18814266]
88. Frid K, Einstein O, Friedman-Levi Y, et al. Aggregation of MBP in chronic demyelination. Ann Clin Transl Neurol. 2015; 2:711–721. [PubMed: 26273684]
89. Wahl SE, McLane LE, Bercury KK, et al. Mammalian target of rapamycin promotes oligodendrocyte differentiation, initiation and extent of CNS myelination. J Neurosci. 2014; 34:4453–65. [PubMed: 24671992]
90. Caron M, Auclair M, Sterlingot H, et al. Some HIV protease inhibitors alter lamin A/C maturation and stability, SREBP-1 nuclear localization and adipocyte differentiation. AIDS. 2003; 17:2437–44. [PubMed: 14600514]
91. Brandmann M, Tulpule K, Schmidt MM, et al. The antiretroviral protease inhibitors indinavir and nelfinavir stimulate Mrp1-mediated GSH export from cultured brain astrocytes. J Neurochem. 2012; 120:78–92. [PubMed: 22017299]
92. Lee DW, Banquy X, Kristiansen K, et al. Lipid domains control myelin basic protein adsorption and membrane interactions between model myelin lipid bilayers. Proc Natl Acad Sci USA. 2014; 111:E768–75. [PubMed: 24516125]
93. Chrast R, Saher G, Nave KA, et al. Lipid metabolism in myelinating glial cells: lessons from human inherited disorders and mouse models. J Lipid Res. 2011; 52:419–34. [PubMed: 21062955]
94. Carr A, Samaras K, Burton S, et al. A syndrome of peripheral lipodystrophy, hyperlipidaemia and insulin resistance in patients receiving HIV protease inhibitors. AIDS. 1998; 12:F51–F8. [PubMed: 9619798]

Author Manuscript Author Manuscript Author Manuscript Author Manuscript

95. Haughey NJ, Cutler RG, Tamara A, et al. Perturbation of sphingolipid metabolism and ceramide production in HIV-dementia. Ann Neurol. 2004; 55:257–67. [PubMed: 14755730]

96. McLaurin JA, Yong VW. Oligodendrocytes and myelin. Neurol Clin. 1995; 13:23–49. [PubMed: 7739504]

97. Kutzelnigg A, Lassmann H. Pathology of multiple sclerosis and related inflammatory demyelinating diseases. Handb Clin Neurol. 2014; 122:15–58. [PubMed: 24507512]

98. Hartley MD, Altowaijri G, Bourdette D. Remyelination and multiple sclerosis: therapeutic approaches and challenges. Curr Neurol Neurosci Rep. 2014; 14:485. [PubMed: 25108747]

99. McKenzie IA, Ohayon D, Li H, et al. Motor skill learning requires active central myelination. Science. 2014; 346:318–22. [PubMed: 25324381]

100. Long P, Corfas G. Neuroscience. To learn is to myelinate. Science. 2014; 346:298–9. [PubMed: 25324370]

101. Blas-Garcia A, Apostolova N, Esplugues JV. Oxidative stress and mitochondrial impairment after treatment with anti-HIV drugs: clinical implications. Curr Pharm Des. 2011; 17:4076–86. [PubMed: 22188456]

102. Roc AC, Ances BM, Chawla S, et al. Detection of human immunodeficiency virus induced inflammation and oxidative stress in lenticular nuclei with magnetic resonance spectroscopy despite antiretroviral therapy. Arch Neurol. 2007; 64:1249–57. [PubMed: 17620480]

103. Gill AJ, Kovacsics CE, Cross SA, et al. Heme oxygenase-1 deficiency accompanies neuropathogenesis of HIV-associated neurocognitive disorders. J Clin Invest. 2014; 124:4459–72. [PubMed: 25202977]

Author Manuscript Author Manuscript Author Manuscript Author Manuscript

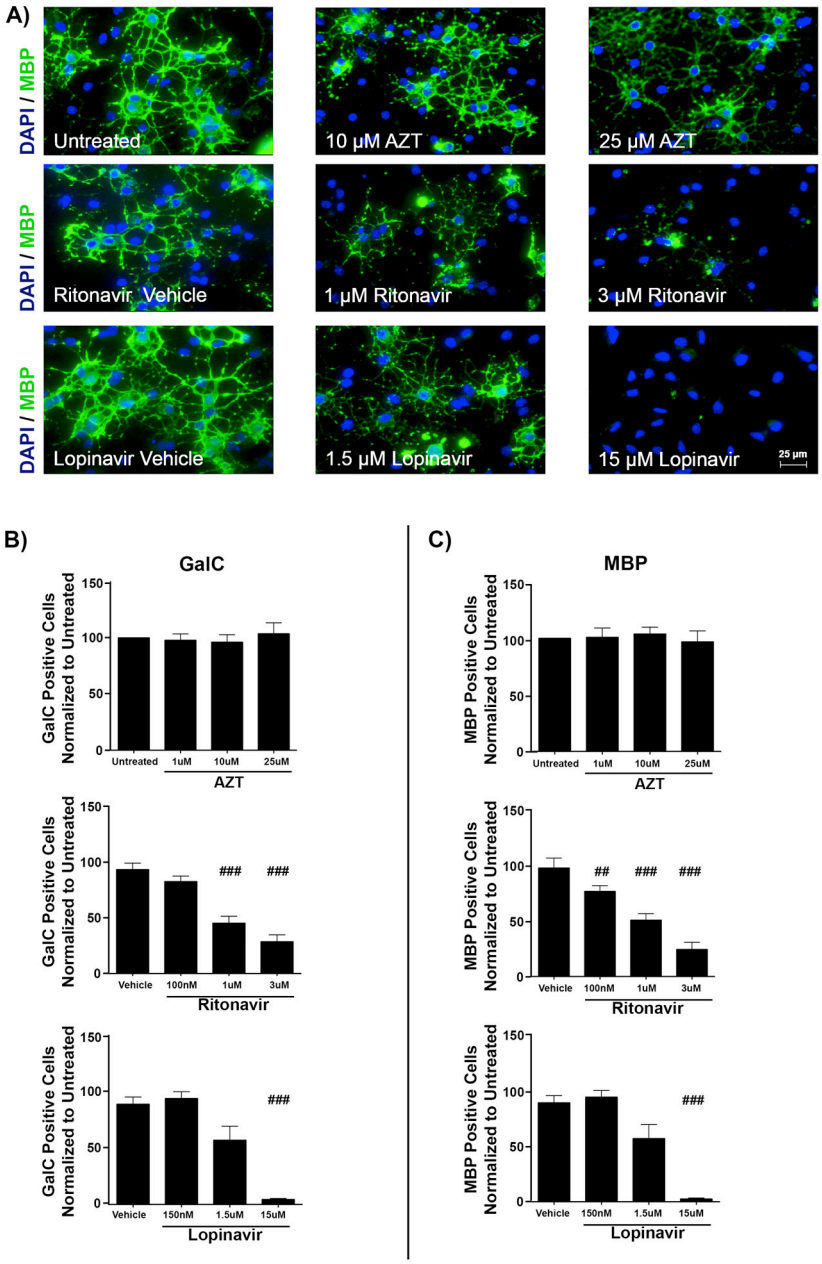

Figure 1.

Antiretrovirals inhibit oligodendrocyte differentiation. Primary mouse oligodendrocyte precursor cells (OPCs) plated on coverslips were put into differentiation medium and treated with vehicle (DMSO), doses of Zidovudine (AZT) (1 μM, 10 μM, or 25 μM), Ritonavir (100 nM, 1 μM, or 3 μM), or Lopinavir (150 nM, 1.5 μM, or 15 μM). After 72 hours, cells were fixed and stained with antibody to myelin basic protein (MBP, green) with DAPI (blue) for total cell nuclei. Epifluorescent images were captured, with 10 fields on 3 coverslips per condition. Results from n = 4 independently prepared cultures. (**A**) Representative images from immunofluorescence staining; scale bar indicates 25 μm. (**B, C**) Immature oligodendrocytes (galactocerebroside [GalC]-positive cells) (**B**) and mature

Author Manuscript Author Manuscript Author Manuscript Author Manuscript

oligodendrocytes (MBP-positive cells) (**C**) were counted using ImageJ software, represented as percentage normalized to untreated. Results from AZT are in the top row, Ritonavir in the center, and Lopinavir in the bottom row, respectively. Data are presented as mean ± SE. One-way ANOVA followed by post-hoc Newman-Keuls determined statistical significance. Significance compared with control (###$p < 0.001$; ##$p < 0.01$).

Author Manuscript Author Manuscript Author Manuscript Author Manuscript

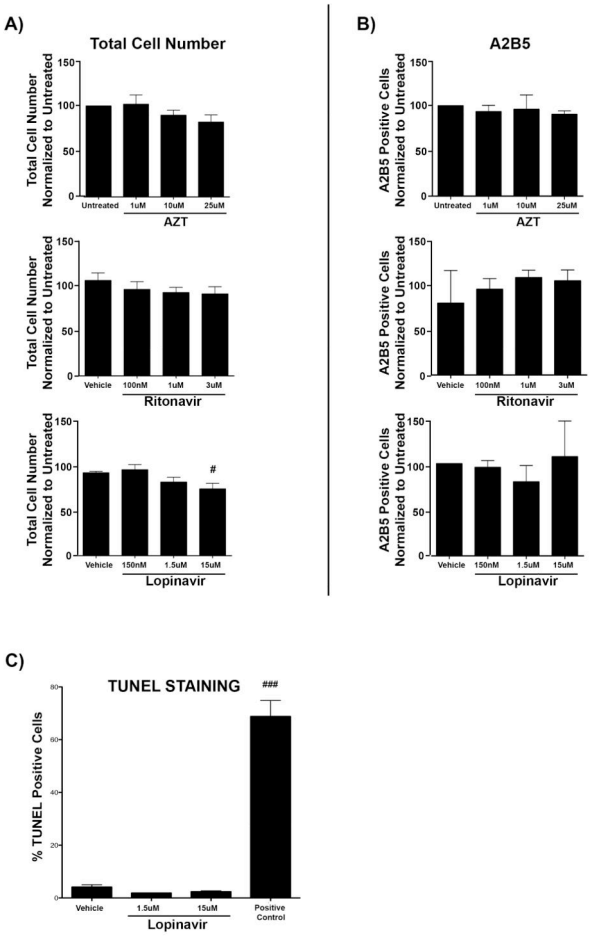

Figure 2.

Antiretrovirals do not alter oligodendrocyte precursor cell (OPC) number or induce apoptotic cell death. (**A, B**) Primary mouse OPCs plated on coverslips were put into differentiation medium and treated with vehicle (DMSO), doses of Zidovudine (AZT) (1 μM, 10 μM, or 25 μM), Ritonavir (100 nM, 1 μM, or 3 μM), or Lopinavir (150 nM, 1.5 μM, or 15 μM). After 72 hours, cells were fixed and stained with antibody to A2B5 with DAPI (blue) for total cell nuclei. Results from AZT are in the top row, Ritonavir in the center, and Lopinavir in the bottom row respectively. Epifluorescent images were captured, with 10 fields on 3 coverslips per condition. (**A**) Total cell number (DAPI-positive nuclei) were counted using ImageJ software from the biological replicates utilized for the dose curves in Figures 1 and 2 (n = 8). Results are represented as percentage normalized to untreated. Significance compared with control (#$p < 0.05$). Data are presented as mean ± SE. One-way ANOVA followed by post-hoc Newman-Keuls determined statistical significance. (**B**) Oligodendrocyte precursor cells (A2B5-positive cells) were counted using ImageJ software and are represented as percentage normalized to untreated. Data are presented as mean ± SE. Results from n = 3 independently prepared cultures. One-way ANOVA followed by post-hoc Newman-Keuls determined statistical significance. (**C**) Primary mouse OPCs plated on coverslips were put into differentiation medium and treated with vehicle (DMSO) or doses of Lopinavir (1.5 μM, or 15 μM). After 72 hours, cells were fixed and stained using a

Author Manuscript Author Manuscript Author Manuscript Author Manuscript

TUNEL assay to label cells with double-stranded DNA breaks indicative of activation of the apoptotic cascade. DNase was used as a positive control. Epifluorescent images were captured at 40x magnification, with 10 fields on 3 coverslips per condition. Results from n= 2 independently prepared cultures. Data are presented as mean ± SE. One-way ANOVA followed by post-hoc Dunnett's comparison determined statistical significance. Significance compared with control (###$p < 0.001$).

Author Manuscript Author Manuscript Author Manuscript Author Manuscript

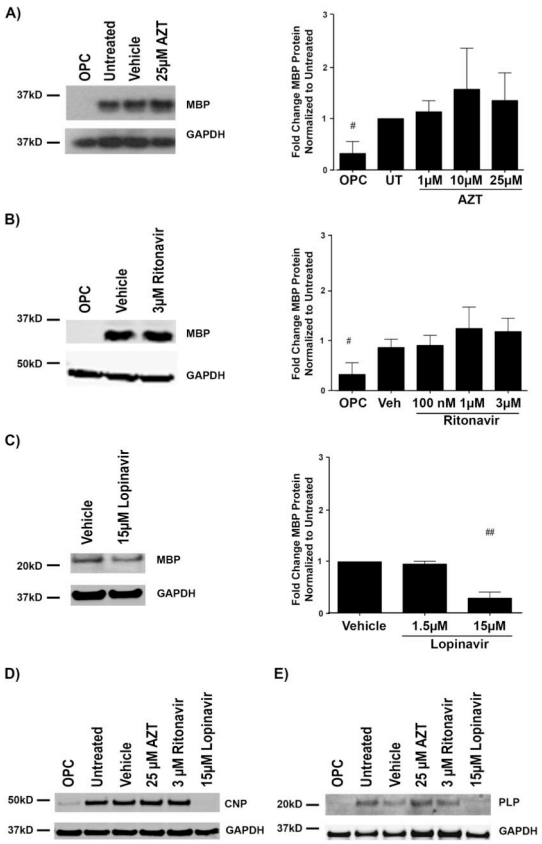

Figure 3.

Lopinavir reduces myelin proteins but zidovudine (AZT) and ritonavir do not. (**A–E**) Oligodendrocyte precursor cells (OPCs) were treated with vehicle, AZT (1 μM, 10 μM, or 25 μM), Ritonavir (100 nM, 1 μM, or 3 μM) or Lopinavir (1.5 μM or 15 μM) at the time of differentiation. After 72 hours, cells were harvested for protein; undifferentiated OPCs were harvested at time 0. Cell lysates were immunoblotted for myelin basic protein (MBP) (**A–C**), cyclic-nucleotide-3′phosphodiesterase (CNPase) (**D**), or proteolipid protein (PLP) (**E**). Representative Western blot image and quantification of band intensities normalized to loading control glyceraldehyde 3-phosphate dehydrogenase (GAPDH) from 5 separate culture groups (n = 5) reveals the typical increase in MBP expression over 72 hours between OPC and untreated, however no significant change with any dose of AZT (**A**). Analysis as in **(A**) from n = 5 reveals the typical increase in MBP expression over 72 hours between OPC and vehicle treatment, however no change with any dose of Ritonavir (**B**). Representative Western blot image and quantification of band intensities normalized to loading control GAPDH from n = 4 reveals treatment with 15 μM Lopinavir resulted in significantly less MBP expression over 72 hours than with vehicle alone or with the lower 1.5 μM dose of Lopinavir (**C**). Representative Western blot images with loading control GAPDH reveals less CNPase expressed at 72 hours following treatment with 15 μM Lopinavir than with the vehicle alone, 25 μM AZT, or 3 μM Ritonavir (**D**). Representative Western blot images with loading control GAPDH reveals less PLP expressed at 72 hours following treatment with 15 μM Lopinavir than with the vehicle alone, 25 μM AZT, or 3 μM Ritonavir. Data are

Author Manuscript Author Manuscript Author Manuscript Author Manuscript

presented as mean ± SE (**E**). One-way ANOVA followed by post-hoc Newman-Keuls determined statistical significance across concentrations. Undifferentiated and Controls (untreated or vehicle) were compared by Student t-test (##$p < 0.01$, #$p < 0.05$).

Author Manuscript Author Manuscript Author Manuscript Author Manuscript

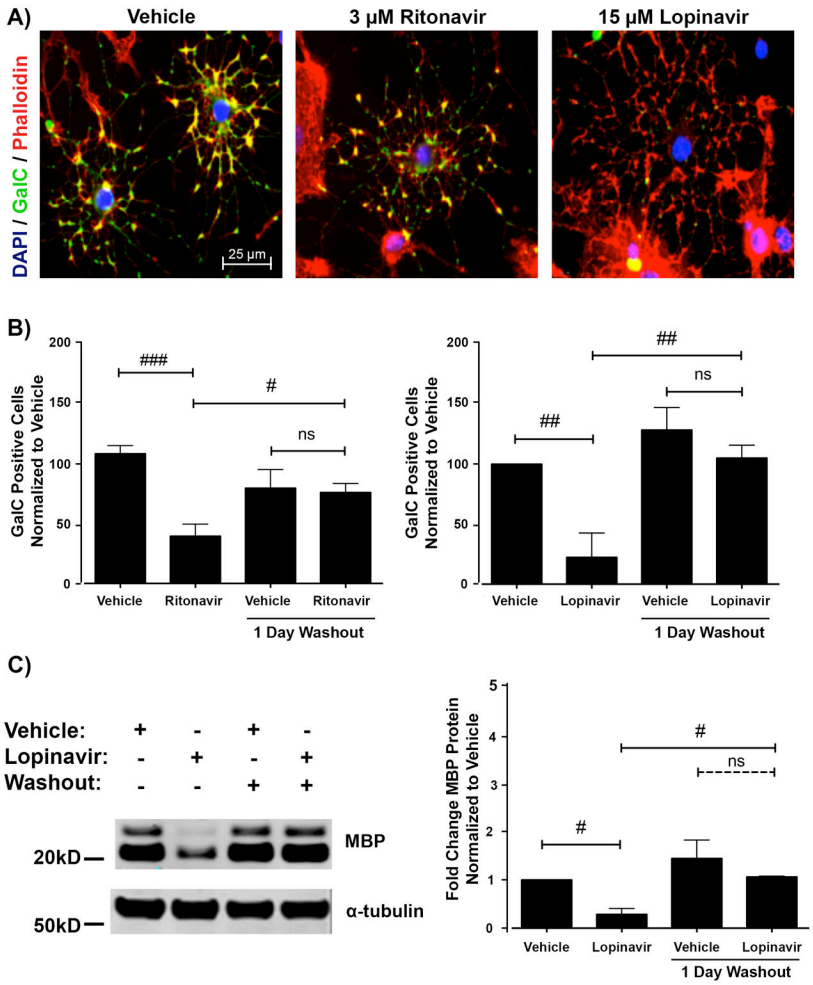

Figure 4.

Antiretroviral inhibition of differentiation is reversible. (**A**) Oligodendrocyte precursor cells (OPCs) were treated with vehicle, 3 μM Ritonavir, or 15 μM Lopinavir at the time of differentiation. After 72 hours, the cells were fixed and stained for galactocerebroside (GalC, green) with DAPI (blue) and Phalloidin (red) for actin. Sample images reveal that cells in Ritonavir and Lopinavir treatments have elaborated morphology but lack the appropriate maturation marker GalC co-staining. Scale bar indicates 25 μm. (**B**) OPCs were treated as in **A**. After 72 hours, the washout group received new differentiation medium without antiretrovirals and was allowed to further mature for 24 hours. Cells were fixed and stained for GalC with DAPI. Cells were counted as in Figure 1 for 15 fields in 3 coverslips per condition at 40x magnification. Data are presented as mean ± SE, n = 4. One-way ANOVA followed by post-hoc Bonferroni correction compared vehicle and treatment conditions at the 2 time points (#$p < 0.05$; ##$p < 0.01$; ###$p< 0.001$, ns, not significant). (**C**) OPCs were treated with vehicle or 15 μM Lopinavir at the time of differentiation. After 72 hours, the washout group received new differentiation medium without treatment and was allowed to further mature for 24 hours. Cell lysates were immunoblotted for MBP protein. Representative Western blot image is shown. Quantification of band intensities normalized to a loading control reveals that Lopinavir-treated cells expressed less MBP protein

Author Manuscript Author Manuscript Author Manuscript Author Manuscript

compared with vehicle; however, this level rose to be comparable to vehicle 24 hours after washout. Data are presented as mean ± SE, n = 3. One-way ANOVA followed by post-hoc Bonferroni correction compared vehicle and treatment conditions at the 2 time points (#$p < 0.05$).

Author Manuscript Author Manuscript Author Manuscript Author Manuscript

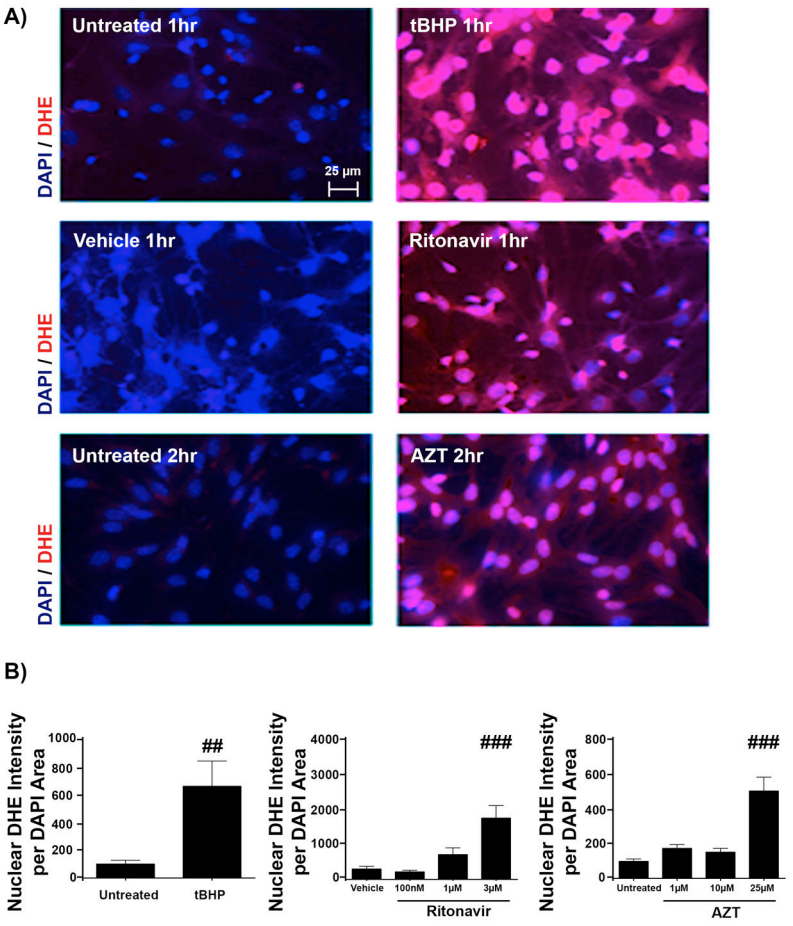

Figure 5.

Antiretrovirals induce oxidative stress. Oligodendrocyte precursor cells (OPCs) were treated with vehicle, Zidovudine (AZT) (1 µM, 10 µM, or 25 µM), Ritonavir (100 nM, 1 µM or 3 µM), Lopinavir (150 nM, 1.5 µM, or 15 µM), or positive control tert-Butyl hydroperoxide (tBHP) (2.5 µM) for 30 minutes, 1 hour, 2 hours, 6 hours, 12 hours, and 24 hours to determine if reactive oxygen species (ROS) were generated. Staining with the superoxide indicator dihydroethidium (DHE) was used as an indicator of ROS, with DAPI staining for cell nuclei. Epifluorescent images were captured at 40x magnification, with 10 fields on 3 coverslips per condition at the time point where ROS began to accumulate for each antiretroviral compound. (**A**) Representative images of 1 hour tBHP- and Ritonavir-treated and 2 hour AZT-treated OPCs, with DHE fluorescence (red) and cell nuclei stained with DAPI (blue). Scale bar indicates 25 µm. In treatments up to 24 hours, Lopinavir produced no accumulation. (**B**) Analysis using Metamorph determined fluorescence intensity of DHE normalized to nuclear DAPI area. Representative experiments are shown; values are presented as mean ± SE, n = 2 for each time point tested. One-way ANOVA followed by post-hoc Newman-Keuls determined statistical significance (##$p < 0.01$; ###$p < 0.001$).

Author Manuscript Author Manuscript Author Manuscript Author Manuscript

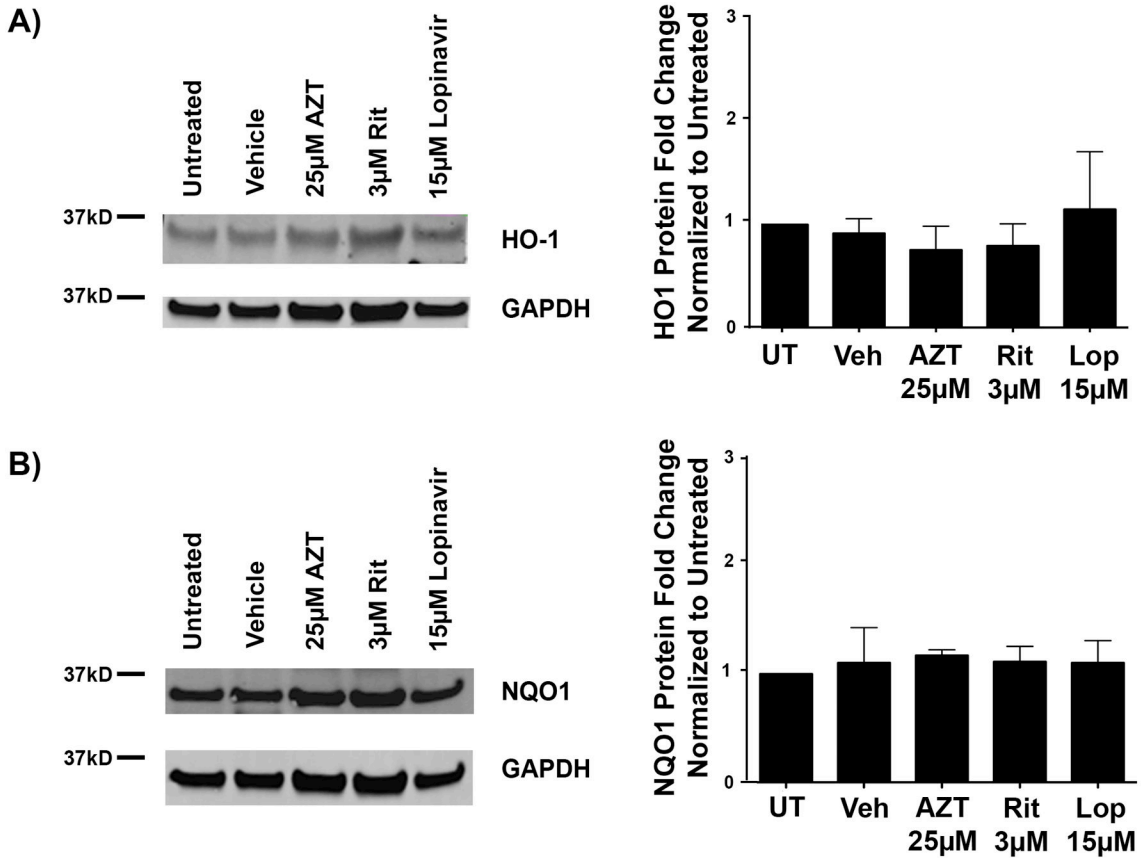

Figure 6.

The endogenous antioxidant response is not triggered by antiretrovirals in developing oligodendrocyte precursor cells (OPCs). (**A, B**) OPCs were treated with vehicle, 25 μM Zidovudine (AZT), 3 μM Ritonavir, or 15 μM Lopinavir at the time of differentiation. After 16 hours, cells were harvested for protein. Cell lysates were immunoblotted for heme oxygenase-1 (HO-1) (**A**) and NAD(P)H:quinone oxidoreductase (NQO1) (**B**), target proteins that are upregulated following activation of the endogenous antioxidant response. Representative Western blot images are shown with quantification of band intensities normalized to glyceraldehyde 3-phosphate dehydrogenase (GAPDH) loading controls revealing no change with any treatment condition. Data are presented as mean ± SE from 3 separate cultures (n = 3). One-way ANOVA followed by post-hoc Dunnett's multiple comparison determined statistical significance.

Author Manuscript Author Manuscript Author Manuscript Author Manuscript

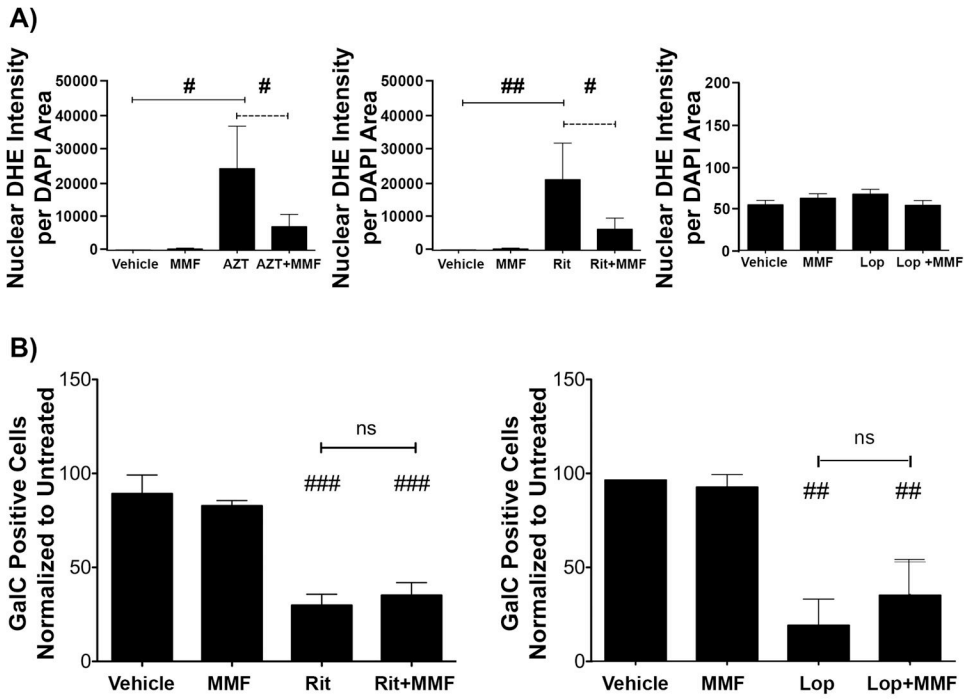

Figure 7.

Effective reduction of reactive oxygen species does not rescue maturation defects. A: Oligodendrocyte precursor cells (OPCs) were pre-treated with 10 μM monomethyl fumarate (MMF) for 6 hours. Cultures were then supplemented with MMF and/or treated with vehicle, 25 μM Zidovudine (AZT) or 3 μM Ritonavir for 2 hours or 15 μM Lopinavir for 6 hours. DHE staining, imaging and analysis was performed as in Figure 4. A representative experiment is shown; values are presented as mean ± SE, n = 2. Student t-test determined significance for direct comparisons (#$p < 0.05$; ##$p < 0.001$). (**B**) OPCs plated on coverslips were pre-treated with 10 μM MMF for 24 hours. Cells were then switched into DM, supplemented with MMF and/or treated with vehicle, 3 μM Ritonavir or 15 μM Lopinavir. MMF was replenished at 24 and 48 hours. After 72 hours, cells were fixed and stained for galactocerebroside (GalC) and DAPI, and were imaged and analyzed as in Figure 1. Data are presented as mean ± SE, from 3 separate cultures (n = 3). Student t-test determined significance for direct comparisons (##$p < 0.01$; ###$p < 0.001$).

Author Manuscript Author Manuscript Author Manuscript Author Manuscript

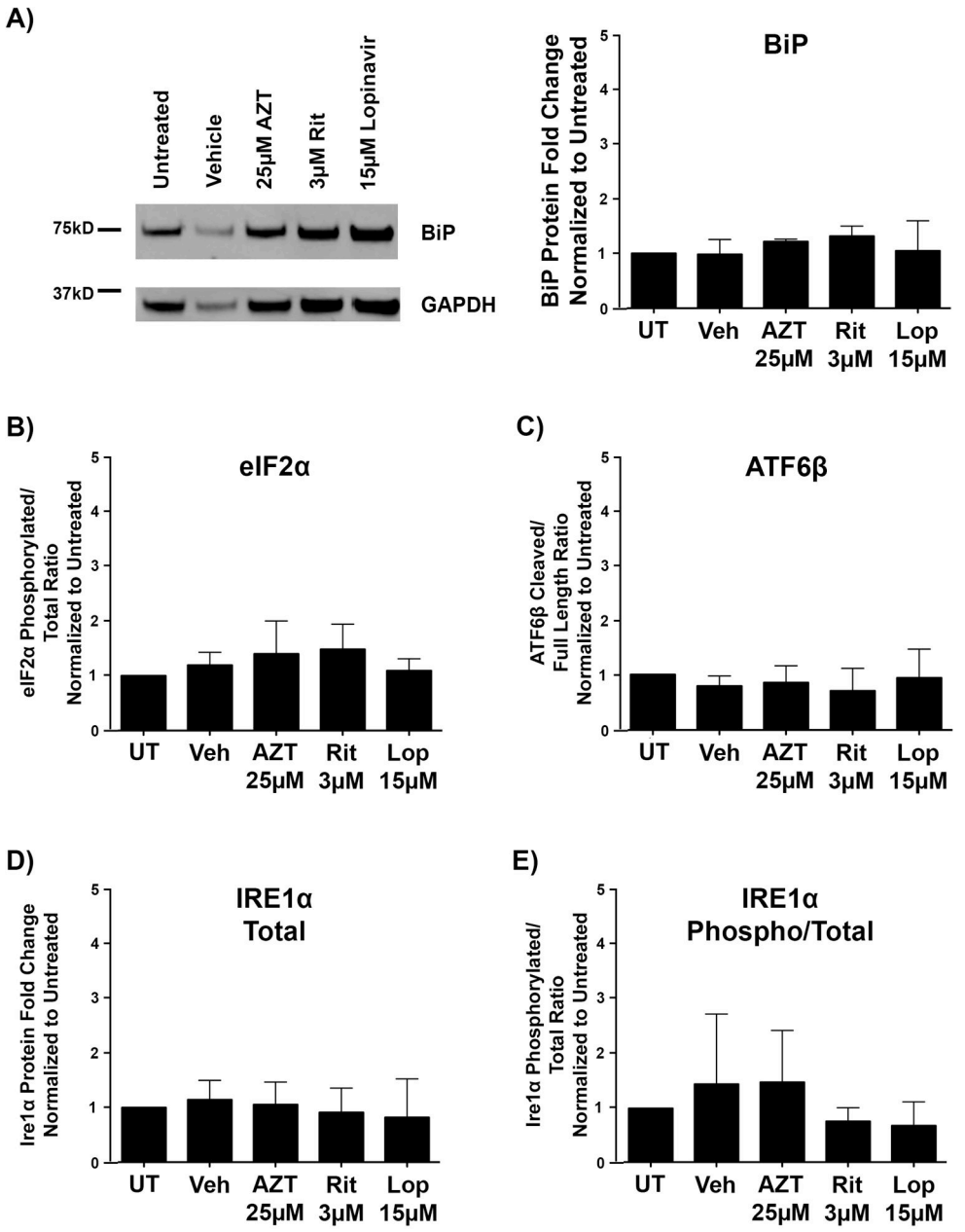

Figure 8.

The unfolded protein response is not triggered by antiretrovirals in developing oligodendrocyte precursor cells (OPCs). OPCs were treated with vehicle, 25 μM Zidovudine (AZT), 3 μM Ritonavir, or 15 μM Lopinavir at the time of differentiation. After 16 hours, cells were harvested for protein. Cell lysates were immunoblotted for protein alterations indicating activation of the unfolded protein response. (**A**) Representative Western blot images of BiP, with quantification of band intensities normalized to glyceraldehyde 3-phosphate dehydrogenase (GAPDH) loading controls from 3 independent biological replicates graphed. (**B–E**) Levels of phosphorylated compared to total eIF2a protein (**B**), cleaved compared to total ATF6β protein (**C**), total IRE1α protein (**D**), and phosphorylated

Author Manuscript Author Manuscript Author Manuscript Author Manuscript

compared to total IRE1α protein (**E**), were each analyzed from 3 separate biological replicates (n = 3). Quantification of band intensities normalized to GAPDH loading controls revealed no changes in any of these proteins following treatment with the antiretrovirals tested. Data are presented as mean ± SE. One-way ANOVA followed by post-hoc Dunnett's multiple comparison test determined statistical significance.

Author Manuscript Author Manuscript Author Manuscript Author Manuscript

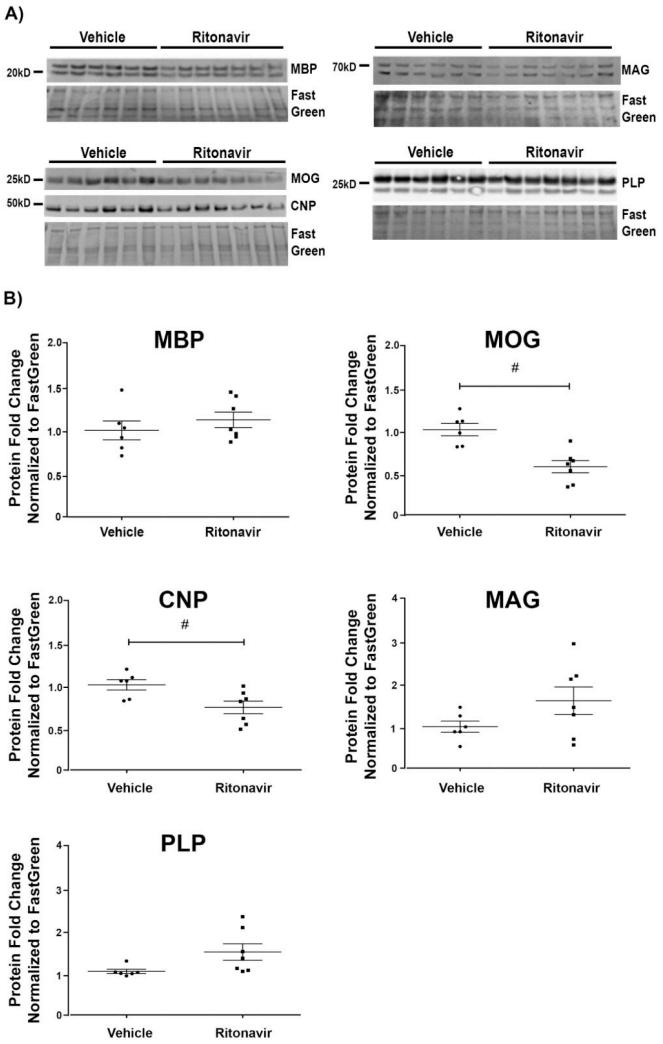

Figure 9.

In vivo ritonavir administration leads to reduction in myelin proteins. Brain lysates derived from our jugular vein administration model were immunoblotted for myelin basic protein (MBP), myelin oligodendrocyte glycoprotein (MOG), cyclic-nucleotide-3′phosphodiesterase (CNP), myelin-associated glycoprotein (MAG), and proteolipid protein (PLP). The drug regimen was composed of vehicle (DMSO) or 20 mg/kg/day of Ritonavir for 14 days. (**A**) Western Blot images from frontal cortex lysates are shown (vehicle n = 6, Ritonavir n = 7). (**B**) Quantification of band intensities normalized to FastGreen FCF reveals statistically significant decreases in MOG and CNP protein levels. Data are presented as mean ± SE. Student t-test determined statistical significance for direct comparisons (#$p < 0.05$).

Author Manuscript Author Manuscript Author Manuscript Author Manuscript

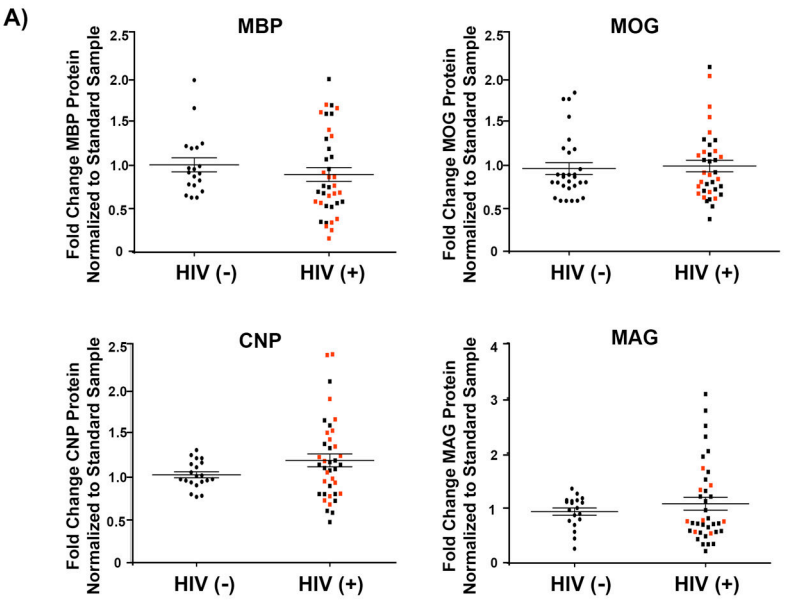

Figure 10.

Myelin protein expression in humans is not affected by HIV status. Lysates from prefrontal cortex specimens of HIV-negative controls [(HIV (−)], and combined HIV-positive antiretroviral therapy cART-naïve and HIV-positive cART-medicated >12 months [HIV-+], were immunoblotted for myelin component proteins myelin basic protein (MBP), myelin oligodendrocyte glycoprotein (MOG), cyclic-nucleotide-3′phosphodiesterase (CNP), and myelin-associated glycoprotein (MAG) (n = 20 for each group). Protein expression levels were determined by quantification of band intensities normalized to a FastGreen total protein loading control. Patient samples were stratified by HIV status with HIV-negative individuals compared with the HIV-positive cases, both cART-naïve and cART-medicated combined, with red data points indicating patients diagnosed with HIV-Associated Neurocognitive Disorders (HAND). Black lines indicate mean ± SE. Student t-test determined statistical significance for direct comparisons, result was not statistically significant.

Author Manuscript Author Manuscript Author Manuscript Author Manuscript

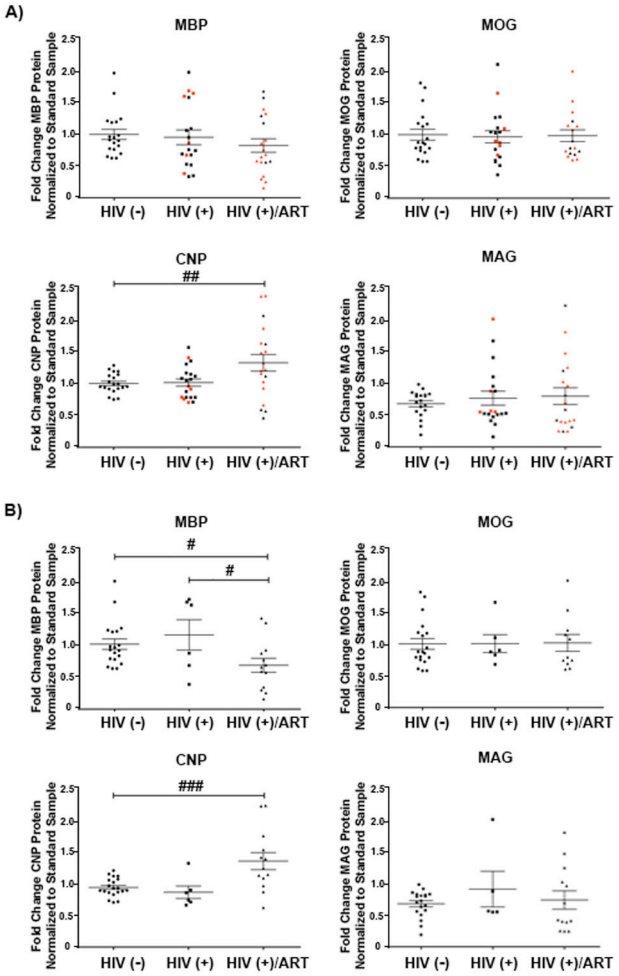

Figure 11.

Myelin protein expression in humans is affected by combined antiretroviral therapy (cART)-medication status. Lysates from prefrontal cortex specimens of HIV-negative controls (n = 20), HIV-positive cART-naïve (n = 20) patients, and HIV-positive cART-medicated >12 months (HIV-positive/ART) patients (n = 20), were immunoblotted for myelin component proteins MBP, MOG, CNP, and MAG. Protein expression levels were determined by quantification of band intensities normalized to a FastGreen total protein loading control. (**A**) Patient samples were stratified by HIV-treatment status, with red data points indicating patients diagnosed with HIV-Associated Neurocognitive Disorders (HAND). Black lines indicate mean ± SE. One-way ANOVA followed by post-hoc Newman-Keuls determined statistical significance (##$p < 0.01$). (**B**) Individuals satisfying criteria for HAND diagnosis were stratified by HIV-treatment status. Black lines indicate mean ± SE. One-way ANOVA followed by post-hoc Newman-Keuls determined statistical significance (#$p < 0.05$; ###$p < 0.001$).

Author Manuscript Author Manuscript Author Manuscript Author Manuscript

Table 1

Patient demographics, Antiretroviral Therapy History and Clinical Data

Characteristic:	HIV-negative	HIV-positive, ART-naïve	HIV-positive ART medicated >12 mo	p value
Number of Subjects	20	20	20	-
Age at death, mean ± SD	42.8 ± 5.6	39.7 ± 7.3	45.3 ± 6.7	0.032[a]
Hours post-mortem, mean ± SD	9.9 ± 5.7	10.0 ± 6.4	12.4 ± 7.9	0.455[a]
Sex				
Male (%)	80%	90%	80%	0.619[b]
Female (%)	20%	10%	20%	
Race				
White (%)	11 (55%)	12 (60%)	15 (75%)	
Black (%)	7 (35%)	8 (40%)	5 (25%)	0.498[b]
Other/Unknown (%)	2 (10%)	0 (0%)	1 (5%)	
Ethnicity				
Hispanic (%)	5 (25%)	3 (15%)	3 (15%)	0.641[b]
Non-Hispanic (%)	15 (75%)	17 (85%)	17 (85%)	
Neurocognitive Impairment Status				
HAND (%)	-	6 (30%)	14 (70%)	
Neuropsych. Impair. Other Origin (%)	-	5 (25%)	4 (20%)	0.009[b]
Neurocognitively Normal (%)	-	1 (5%)	2 (10%)	
No Neurocognitive Data (%)	-	8 (40%)	0 (0%)	
ARV Treatment Status				
PI-Experienced (%)	-	-	17 (85%)	
PI-Naïve (%)	-	-	3 (15%)	
NRTI-Experienced (%)	-	-	20 (100%)	
NRTI-Naïve (%)	-	-	0 (0%)	
Disease Parameters				
HIVE (%)	-	6 (30%)	1 (5%)	
Log Plasma HIV c/mL, mean ± SD	-	4.1 ± 1.4	4.7 ± 1.1	0.196[c]
Log Brain HIV g/mL, mean ± SD	-	3.4 ± 1.9	4.1 ± 0.9	0.358[c]
Log CSF HIV c/mL, mean ± SD	-	3.4 ± 1.8	2.8 ± 1.1	0.261[c]
$CD4^+$ lymphocytes/mm^3, mean ± SD	-	108 ± 118	85 ± 118	0.624[c]

ART, antiretroviral Therapy; ARV, antiretroviral; HAND, HIV-Associated Neurocognitive Disorders; Neuropsych. Impair., neuropsychiatric impairment; PI, HIV protease inhibitor; NRTI, nucleoside reverse transcriptase inhibitor, HIVE, HIV encephalitis; mo, months.

[a] Analysis of Variance (ANOVA) p value.

[b] Chi-square test p value.

[c] Student t-test p value.

Author Manuscript

Author Manuscript

Author Manuscript

Author Manuscript

Table 2

Primers Used for q-RT PCR

Gene:	Primer Sequences:
PKG1	Forward: 5′ ATG CAA AGA CTG GCC AAG CTA C 3′
	Reverse: 5′ AGC CAC AGC CTC AGC ATA TTT C 3′
HO-1	Forward: 5′ TGT AAG GGA GAA TCT TGC CTG GCT 3′
	Reverse: 5′ TGC TGG TTT CAA AGT TCA GGC CAC 3′
NQO1	Forward: 5′ AAG AGC TTT AGG GTC GTC TTG GCA 3′
	Reverse: 5′ AGC CTC CTT CAT GGC GTA GTT GAA 3′
XBP-1 Spliced	Forward: 5′ GAG TCC GCA GCA GGT G 3′
	Reverse: 5′ GCT TAG AGG TGC TTC CTC AAT 3′
XBP-1 Total	Forward: 5′ CAC CTC TGC AGC AGG TG 3′
	Reverse: 5′ GCT TAG AGG TGC TTC CTC AAT 3′
BiP	Forward: 5′ TGG ATA AGA GAG AGG GAG AGA AG 3′
	Reverse: 5′ GTG AGA AGA GAC ACA TCG AAG G 3′
CHOP	Forward: 5′ CAG CGA CAG AGC CAG AAT AA 3′
	Reverse: 5′ CAG GTG TGG TGG TGT ATG AA 3′
Ire1α	Forward: 5′ TCC TAA CAA CCT GCC CAA AC 3′
	Reverse: 5′ TCT CCT CCA CAT CCT GAG ATA C 3′
ATF6	Forward: 5′ CTC GGC TCG GTA GTT TGT ATC 3′
	Reverse: 5′ AGA CCT GAA TGG CTG CTT AC 3′
ATF4	Forward: 5′ CCA CTC CAG AGC ATT CCT TTA G 3′
	Reverse: 5′ CTC CTT TAC ACA TGG AGG GAT TAG 3′

Primer pairs used for qRT-PCR obtained from Integrated DNA Technologies (Coralville, IA) are shown.

Abbreviations are: PKG1, Protein Kinase Gene 1; HO-1, Heme Oxygenase-1; NQO1, NAD(P)H:quinone oxidoreductase; XBP-1, X-box Binding Protein 1; BiP, Binding Immunoglobulin Protein; CHOP, C/EBP homologous protein; Ire1α, inositol-requiring enzyme 1 alpha; ATF6, activating transcription factor 6; ATF4, activating transcription factor 4.

Author Manuscript

Author Manuscript

Author Manuscript

Author Manuscript

Table 3

mRNA alterations in Endogenous Antioxidant Response Genes Following Antiretroviral Application in Primary Oligodendrocyte Precursor Cells

Gene	Treatment	ΔΔCT ± SE	Fold Change Relative to Control	P value
HO-1	AZT	−0.639 ± 1.356	1.558 (0.609–3.987)	0.3503
	Ritonavir	1.116 ± 1.363	0.461 (0.179–1.187)	0.9402
	Lopinavir	0.6117 ± 0.9833	0.654 (0.331–1.294)	<0.0001 *
NQO1	AZT	−0.14 ± 2.714	1.102 (0.168–7.230)	0.7153
	Ritonavir	−0.780 ± 0.221	1.716 (1.473–2.00)	0.015 *
	Lopinavir	−0.195 ± 1.2	1.272 (0.554–2.921)	<0.0001 *

Extracted RNA (5 μg) was converted to cDNA using the Superscript First-strand kit and q-PCR was performed using Power SYBR Green. All measurements were normalized first to the oligodendrocyte housekeeping gene PKG1, and then to controls. Analysis was performed by the ΔΔCT method. Endogenous Antioxidant Response genes: HO-1 and NQO1 were probed. ΔΔCT ± SE, fold change, and fold change range are presented from 3 independent biological replicates (n = 3). P values are indicated;

* $p < 0.05$. AZT, Zidovudine.

Author Manuscript Author Manuscript Author Manuscript Author Manuscript

Table 4

mRNA Alterations in Unfolded Protein Response Genes Following Antiretroviral Application In Primary Oligodendrocyte Precursor Cells

Gene	Treatment	ΔΔCT ± SE	Fold Change Relative to Control	P value
XBP-1 Spliced/Total Ratio	AZT	2.991 ± 0.841	0.126 (0.070–0.225)	0.1414
	Ritonavir	0.7938 ± 0.4721	0.577 (0.416–0.800)	0.705
	Lopinavir	1.328 ± 0.4233	0.398 (0.297–0.534)	<0.0001 *
BiP	AZT	−0.662 ± 0.736	1.582 (0.095–2.635)	0.4630
	Ritonavir	0.8850 ± 0.643	0.541 (0.347–0.846)	0.3023
	Lopinavir	−0.7450 ± 0.558	1.676 (1.138–2.467)	0.4094
CHOP	AZT	−0.4083 ± 0.482	1.327 (0.950–1.853)	0.5523
	Ritonavir	0.7886 ± 1.029	1.727 (0.847–3.525)	0.5236
	Lopinavir	0.2650 ± 0.868	0.8832 (0.456–0.658)	0.8114
Ire1α	AZT	2.214 ± 2.021	0.216 (0.053–0.875)	0.4710
	Ritonavir	−0.0517 ± 1.572	1.036 (0.349–3.082)	0.9791
	Lopinavir	−3.115 ± 0.022	8.664 (8.532–8.797)	0.004 *
ATF6	AZT	−0.8156 ± 2.000	1.760 (0.440–7.040)	0.7225
	Ritonavir	0.2694 ± 0.664	0.830 (0.524–1.315)	0.7242
	Lopinavir	0.5700 ± 1.047	0.674 (0.326–1.392)	0.6825
ATF4	AZT	−1.307 ± 0.435	2.474 (1.830–3.345)	0.0953
	Ritonavir	0.2317 ± 0.753	0.852 (0.505–1.435)	0.7875
	Lopinavir	−0.0650 ± 0.892	1.046 (0.981–1.115)	0.9537

Extracted RNA (5 μg) was converted to cDNA using the Superscript First-strand kit and q-PCR was performed using Power SYBR Green. All measurements were normalized first to the oligodendrocyte housekeeping gene PKG1, and then to controls. Analysis was performed by the ΔΔCT method. Unfolded Protein Response genes: *XBP-1* spliced, *XBP-1* total, *BiP*, *CHOP*, *Ire1α*, *ATF6*, and *ATF4* were probed. ΔΔCT ± SE, fold change, and fold change range are presented from 3 independent biological replicates (n = 3). P values are indicated;

* $p < 0.05$. AZT, Zidovudine.